



Contents lists available at ScienceDirect

Gondwana Research

journal homepage: www.elsevier.com/locate/gr

Q4 Zircon U–Pb ages of rocks from the Rio Apa Cratonic Terrane
 2 (Mato Grosso do Sul, Brazil): New insights for its connection
 3 with the Amazonian Craton in pre-Gondwana times

Q5 F.M. Faleiros^{a,b,*}, M. Pavan^a, M.J. Remédio^a, J.B. Rodrigues^c, V.V. Almeida^a, F.P. Caltabeloti^a, L.G.R. Pinto^a,
 5 A.A. Oliveira^a, E.J. Pinto de Azevedo^a, V.S. Costa^a

6 ^a Geological Survey of Brazil (CPRM), Regional Superintendence of São Paulo, Rua Costa 55, São Paulo, SP 01304-010, Brazil

7 ^b Instituto de Geociências, Universidade de São Paulo, Rua do Lago, 562, Cidade Universitária, São Paulo, SP 05508-010, Brazil

8 ^c Geological Survey of Brazil (CPRM), SGAN 603, Conjunto J, Parte A, 1° andar, Brasília-DF 70830-030, Brazil

ARTICLE INFO

Article history:

Received 22 July 2014

Received in revised form 20 February 2015

Accepted 24 February 2015

Available online xxx

Handling Editor: J.G. Meert

Keywords:

Rio Apa Craton

Amazonian Craton

Proterozoic supercontinents

Zircon U–Pb geochronology

Tectonic evolution

ABSTRACT

This paper presents 14 zircon U–Pb determinations (SHRIMP and LA-MC-ICP-MS) for key geological units from the Rio Apa Cratonic Terrane (RACT), which is considered the southernmost exposed part of the Amazonian Craton in southwestern Brazil. The zircon U–Pb ages and geological data indicate that the RACT was formed by the accretion of magmatic arcs in a continental margin active from 1950 to 1720 Ma. The RACT is composed of three major terranes (Western, Eastern and Southeastern Terranes) with distinct evolution histories. The Western Terrane presents orthogneisses and granites formed at ~1950–1940 Ma and subduction-related granites and volcanic rocks formed at 1900–1880 Ma and 1840–1830 Ma. These basement rocks are covered by a greenschist facies metavolcano-sedimentary succession (Rio Naicata Formation) with basal volcanic rocks formed at 1813 ± 18 Ma. A gabbro-noritic dyke of the Rio Perdido Suite hosted by the Rio Naitaca Formation yields an age of 1589 ± 44 Ma. The Eastern and Southeastern Terranes present deformed leucogranites generated within the intervals 1780–1720 Ma and 1810–1790 Ma, respectively. Both terranes are covered by a metavolcano-sedimentary succession (Alto Tererê Formation) dominated by Barrovian-type amphibolite facies metamorphic assemblages, suggestive of a collisional event. Available ⁴⁰Ar–³⁹Ar data (hornblende, muscovite and biotite) indicate that the proto-RACT evolved to a collisional orogen between 1310 and 1270 Ma and behaved as a cratonic mass after 1270 Ma, preceding the assembly of Rodinia. The available data allow us to interpret the RACT as a part of the Ventuari–Tapajós Province of the Amazonian Craton, which was fragmented and dispersed as a microcontinent. It was subsequently reincorporated into the SW Amazonian Craton, along the Sunsás Belt, as an allochthonous terrane. In a global perspective, the tectono-magmatic events of the RACT are consistent with a long-lived accretionary orogen possibly related to an active margin of Columbia.

© 2015 Published by Elsevier B.V. on behalf of International Association for Gondwana Research.

1. Introduction

The Rio Apa Cratonic Terrane (RACT; Fig. 1) is a composite terrane that is considered the southernmost exposed part of the Amazonian Craton in southwestern Brazil (Mato Grosso do Sul State) and northern Paraguay (Ruiz et al., 2005; Lacerda Filho et al., 2006; Cordani et al., 2009; Godoy et al., 2009; Cordani et al., 2010a; Manzano et al., 2012; Brittes et al., 2013; Manzano, 2013; Plens et al., 2013; Teixeira et al., 2013). Thus, its evolutionary history is relevant to the reconstruction of the Gondwana and Rodinia supercontinents. The RACT–Amazonia connection is largely based on the positions of the Neoproterozoic Brasiliano/Pan African belts (Almeida and Hasui, 1984) and on the interpretation that the Tucavaca Belt, a Brasiliano feature that separates

the RACT from the Amazonian Craton (Fig. 1), represents an aulacogenic feature (Brito Neves et al., 1985; Ávila-Salinas, 1992; Cordani et al., 2009, 2010a). Although the RACT–Amazonia connection within Gondwana is generally accepted, the pre-Gondwana relationship between these geotectonic entities is not yet properly understood.

Geochronological and geological data suggest that the RACT comprises a fragment of an Orosirian to Statherian active continental margin that was subsequently deformed and metamorphosed in a 1310–1270 Ma collisional event (Lacerda Filho et al., 2006; Cordani et al., 2010a; Manzano et al., 2012; Brittes et al., 2013; Manzano, 2013; Plens et al., 2013; Pavan and Faleiros, 2014). ⁴⁰Ar–³⁹Ar data (muscovite and biotite) indicate that the RACT behaved as a cratonic mass after 1310–1270 Ma (Cordani et al., 2010a) and was unaffected by tectonothermal events related to the assembly of Rodinia (ca. 1200–1000 Ma) and Gondwana (ca. 650–500 Ma). In this scenario, the role of prominent structures related to the Grenvillian Orogeny

Q6 * Corresponding author at: Instituto de Geociências, Universidade de São Paulo, Brazil.
 E-mail address: ffalei@usp.br (F.M. Faleiros).

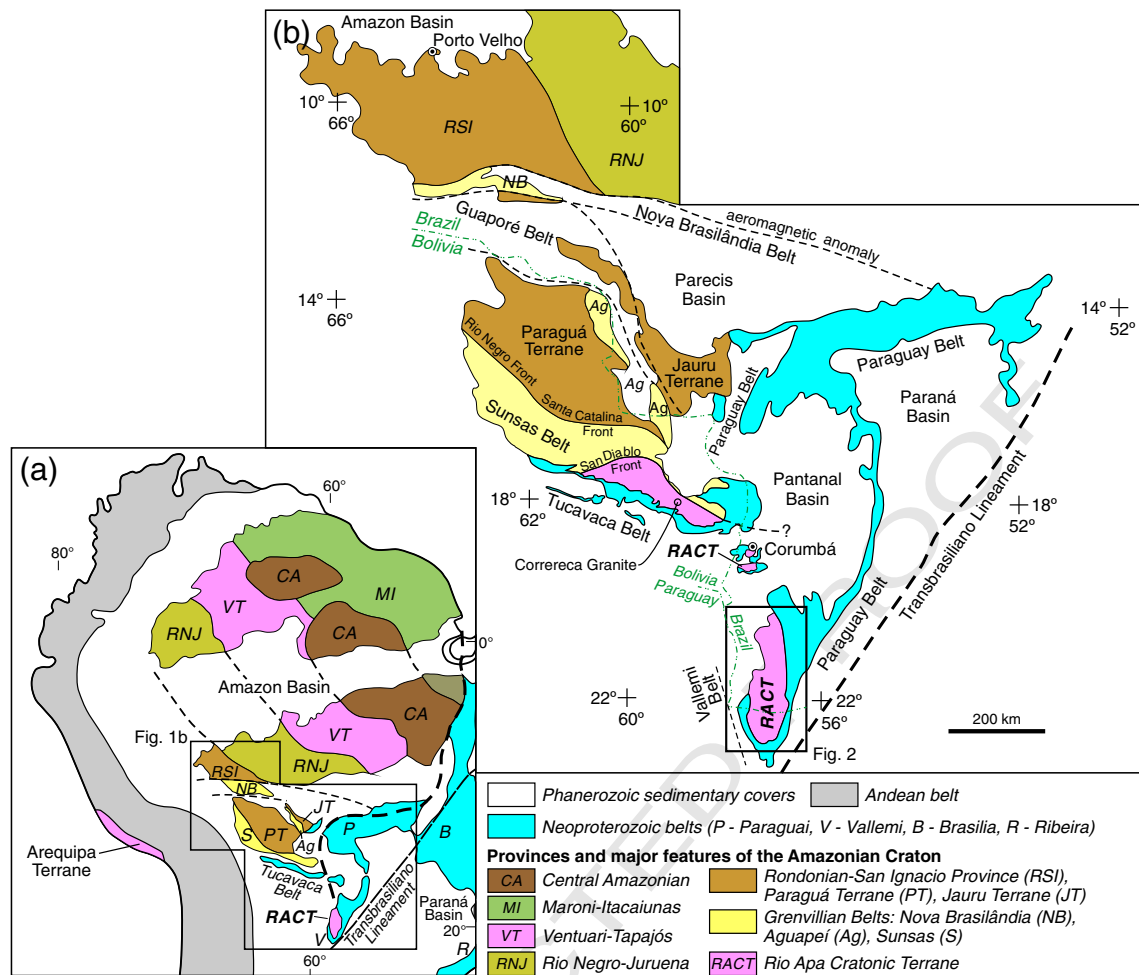


Fig. 1. Tectonic framework of part of South America with emphasis on the Amazonian Craton and its tectonic provinces: (a) adapted from Cordani et al. (2009), (b) adapted from Bettencourt et al. (2010), taking into account data from Hasui and Almeida (1970), Tohver et al. (2004), Vargas-Mattos et al. (2010), Rizzotto et al. (2013) and this work. Also shown is the location of Fig. 2.

(1200–1000 Ma) (the Sunsás, Aguapeí and Nova Brasilândia Belts; Sadowski and Bettencourt, 1996; Geraldès et al., 1997, 2001; Loewy et al., 2004; Tohver et al., 2004; Boger et al., 2005; Tohver et al., 2005a, b, 2006; Teixeira et al., 2010; Geraldès et al., 2014; Rizzotto et al., 2014) and the Rondonian–San Ignacio Orogeny (1560–1300 Ma) (the Guaporé Belt; Bettencourt et al., 2010; Rizzotto et al., 2013, 2014) are key issues that need to be addressed to securely establish the relationship between the RACT and the Amazonian Craton in pre-Gondwana times. Most authors consider the Sunsás Belt as a major suture zone related to the collision between the proto-Amazonian Craton and the Arequipa–Antofalla Terrane (Sadowski and Bettencourt, 1996; Loewy et al., 2004; Boger et al., 2005; Cordani et al., 2010b; Teixeira et al., 2010; Rizzotto et al., 2014), while others interpret it as an intracontinental belt (Santos et al., 2000, 2008). The role of the Nova Brasilândia Belt is also contentious, being inferred as the collisional suture zone between the Paraguá Terrane and the proto-Amazonian Craton (Tohver et al., 2004, 2005a,b, 2006; Boger et al., 2005) or as an intracontinental belt (Santos et al., 2000, 2008; Teixeira et al., 2010; Rizzotto et al., 2014). Rizzotto et al. (2013, 2014) interpret the collage between the Paraguá Terrane (Fig. 1) and the proto-Amazonian Craton to have occurred between 1430 and 1340 Ma along the Guaporé Belt.

In addition to Rodinia and Gondwana, the age (1950–1750 Ma) and tectonic setting of magmatic events recorded in the RACT basement (Lacerda Filho et al., 2006; Cordani et al., 2010a; Brittes et al., 2013; Plens et al., 2013) make its evolutionary history potentially relevant to the reconstruction of the Columbia supercontinent (Meert, 2002;

Rogers and Santosh, 2002; Zhao et al., 2002, 2004, 2011; Roberts, 2012, 2013; Meert, 2014). However, this history has not been taken into account in recent Columbia reconstructions based on paleomagnetic data (Bispo-Santos et al., 2008, 2012, 2014a,b). The only exception is the Columbia reconstruction presented by Teixeira et al. (2013), where the RACT appears in a marginal position, suggesting that it was part of the proto-Amazonian Craton at ca. 1790 Ma.

The tectonic evolution of the RACT is reviewed by Cordani et al. (2010a). New data were recently obtained from systematic geological mapping at a 1:100,000 scale (Remédio et al., 2013; Faleiros et al., 2014; Pavan et al., 2014; Pinto-Azevedo et al., 2014). These data enable refinement of our understanding about the tectonic evolution of the RACT, with implications for the evolution of Proterozoic supercontinents (Columbia and Rodinia). In this paper we report 14 zircon U–Pb data obtained from magmatic rocks of different units from the RACT, eight analyses performed by sensitive high-resolution ion microprobe (SHRIMP), and six analyses by laser ablation-multicollector-inductively coupled plasma mass spectrometry (LA-MC-ICP-MS). These robust geochronological data were used to: (i) contribute to the recognition of terranes with distinct evolution histories prior to amalgamation of the RACT; (ii) understand the relationships between granitoids and supracrustal rocks that present ambiguous contact relationships; (iii) better recognize distinct magmatic events and their tectonic implications; and (iv) contribute to the understanding of the RACT–Amazonia connection history in pre-Gondwana times. The results from this work also aid in our understanding of Paleo-Mesoproterozoic-

aged accretionary processes and the formation of the Columbia and Rodinia supercontinents.

2. Geological setting

Outcrops of the RACT are poor and are typically covered by Quaternary sediments of the Pantanal Formation (Fig. 2). The RACT extends from Mato Grosso do Sul State in southwestern Brazil to northern Paraguay. It presents a N–S-trending peninsular shape, with its eastern–southern–southwestern margins covered in an erosive unconformity

by an Ediacaran cratonic cover of equivalent units, namely, the Corumbá Group (Boggiani, 1997; Campanha et al., 2011) in Brazil and the Itapucumi Group (Warren, 2011; Warren et al., 2011) in Paraguay. The Corumbá and Itapucumi Groups consist of a 400–700-meter-thick succession with conglomerate, sandstone and pelite at the base, passing into dolomite, limestone and carbonaceous pelite on top, and finally covered by a thick pelitic package (Boggiani, 1997; Campanha et al., 2011; Warren, 2011; Warren et al., 2011). A sample of tuff from the Corumbá Group yields a zircon U–Pb SHRIMP age of 543 ± 2 Ma, interpreted as the time of crystallization of the rock and of the

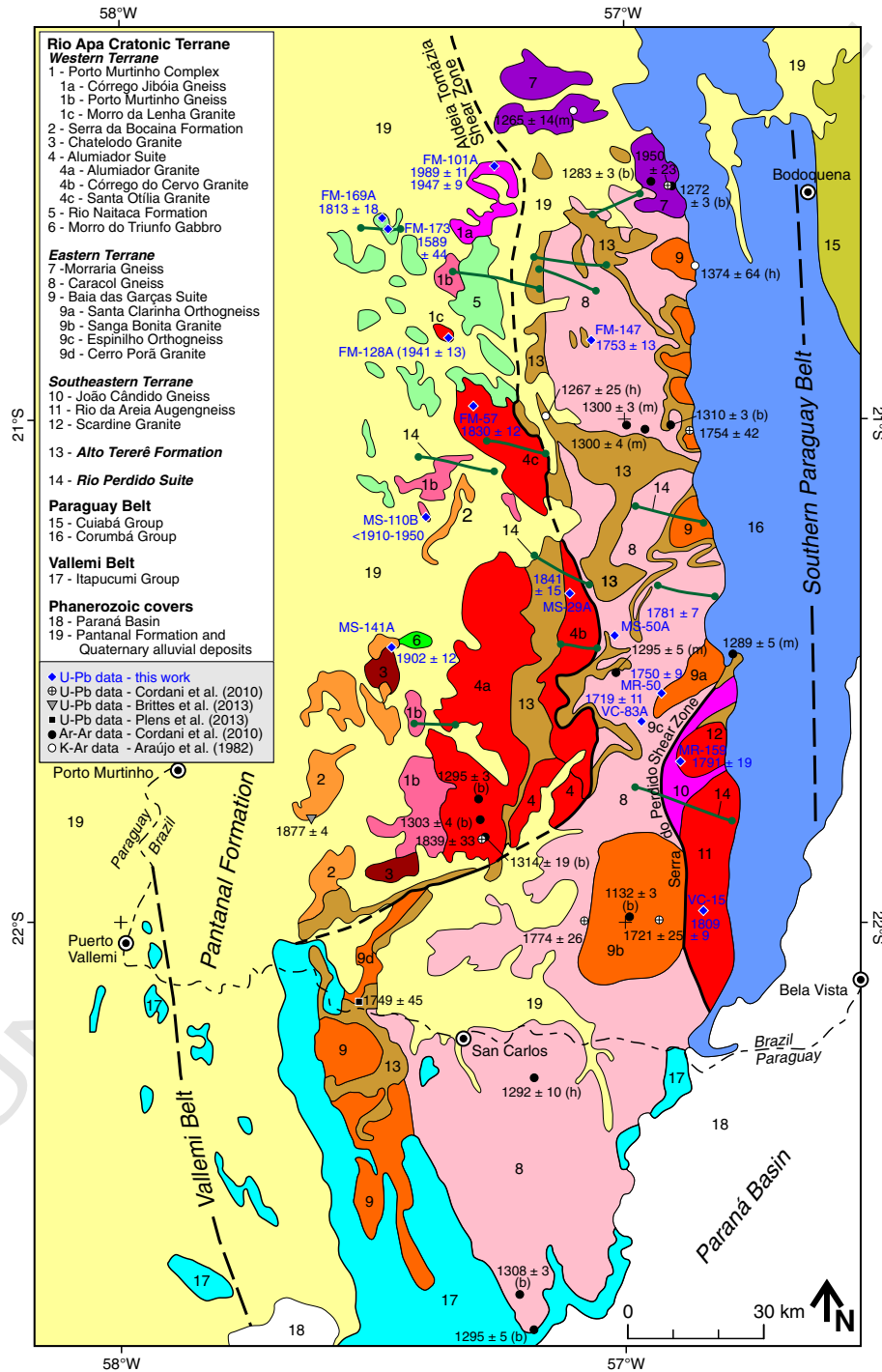


Fig. 2. Simplified geological map of the Rio Apa Cratonic Terrane. Also shown are the locations and ages of samples with zircon U–Pb data from this work, Cordani et al. (2010a, 2010b), Brittes et al. (2013) and Plens et al. (2013), ^{40}Ar – ^{39}Ar data from Cordani et al. (2010a) and K–Ar data from Araújo et al. (1982). Mineral abbreviations for ^{40}Ar – ^{39}Ar and K–Ar data are used as follows: h: hornblende, b: biotite, m: muscovite.

sedimentation of the Corumbá Group (Babinski et al., 2008). The Corumbá Group shows an easterly increase in intensity of deformation and metamorphism due to the activity in the southern Paraguay Belt, which evolved as a typical fold-and-thrust belt with westward vergence (Campanha et al., 2011). In its eastern portion, the Corumbá Group covers the Cuiabá Group, which is dominated by metapelites (phyllite and schist) inferred as of turbiditic origin (Boggiani, 1997). The westernmost portion of the Itapucumi Group in Paraguay was deformed and metamorphosed in the Vallemi Belt. The Vallemi Belt shows a structural vergence opposite that of the Paraguay Belt (Campanha et al., 2010; Warren, 2011). The Vallemi Belt is very poorly exposed, being largely covered by Quaternary sediments equivalent to the Pantanal Formation (Warren, 2011).

The relationship between the RACT and the Amazonian Craton is obscured due to the Ediacaran and Phanerozoic covers (Fig. 1). Furthermore, the tectonic significance of the Grenvillian-age belts (Sunsás, Aguapeí and Nova Brasilândia) is the main limiting factor for possible reconstructions. Based on the geochronology and tectonic setting of granitic magmatism, Cordani et al. (2010a) correlate the RACT with the Rio Negro–Juruena Province of the Amazonian Craton (Tassinari and Macambira, 1999). The available geological data raise two other possibilities: (i) the RACT is a prolongation of the Paraguá or Jauru Terranes, or (ii) the RACT was juxtaposed with the Paraguá and Jauru Terranes along the Sunsás Belt as an allochthonous terrane. The first two hypotheses are favored by the models where the Sunsás, Aguapeí and Nova Brasilândia Belts are interpreted as intracontinental features (Santos et al., 2000, 2008; Rizzotto et al., 2014). In contrast, the third hypothesis is favored by models where the Sunsás and/or Nova Brasilândia Belts are inferred as collisional suture zones (Sadowski and Bettencourt, 1996; Loevy et al., 2004; Tohver et al., 2004; Boger et al., 2005; Tohver et al., 2005a,b, 2006; Teixeira et al., 2010). The question of interrelationships between the Grenvillian-age belts is also contentious, and it has implications for possible tectonic reconstructions. Tohver et al. (2004, 2005a, 2005b, 2006) interpret the Nova Brasilândia Belt as a 2000-km-long suture zone (Fig. 1), and they consider the Aguapeí Belt as an independent intracontinental structure. In contrast, Boger et al. (2005) interpret the two structures as segments of a continuous collisional belt. Geological and geochronological data (Saes, 1999; Gerales et al., 2001; Matos et al., 2004; Tohver et al., 2004, 2006; Ruiz et al., 2005; Rizzotto et al., 2013, 2014) suggest that the Paraguá and Jauru Terranes behaved as a single continent after ca. 1300 Ma, favoring an intracontinental origin for the Aguapeí Belt. Furthermore, Rizzotto et al. (2013) present evidence that the Paraguá and Jauru Terranes were juxtaposed along the Guaporé Belt (Fig. 1), a feature that evolved from an accretionary to a collisional orogen from 1470–1430 Ma to 1430–1340 Ma, respectively.

The granitic basement that outcrops at the Corumbá adjacencies is commonly considered the northernmost exposed portion of the RACT (Fig. 1). This basement presents K–Ar ages of 1730 ± 22 Ma (biotite) and 889 ± 44 Ma (K-feldspar) (Häsui and Almeida, 1970). These data indicate that this basement has not undergone tectonothermal effects related to the Rondonian–San Ignacio event (1560–1300 Ma), and it was possibly slightly affected by the late Sunsás event, as the closure temperature of K-feldspar to the argon system can be as low as 150 °C (Lovera et al., 1989).

Casquet et al. (2009, 2012) interpret the RACT to be part of another cratonic mass (Mara Craton) during the Paleoproterozoic, and it was attached to the Amazonian Craton through the Rondonian–San Ignacio Orogen. The Mara Craton would be made up of the Maz Terrane (Western Sierras Pampeanas, Argentina), the Arequipa Terrane (Peru) and the RACT (Brazil and Paraguay). This model also implies the absence of Grenvillian-age suture zones in the SW Amazonian Craton.

Fig. 2 shows an updated geological map of the RACT that incorporates information of maps at the 1:100,000 scale (Remédio et al., 2013; Faleiros et al., 2014; Pavan et al., 2014; Pinto-Azevedo et al., 2014). The RACT is primarily composed of Paleoproterozoic rocks

divided into four main lithological conjuncts: granitic gneisses, undeformed to slightly deformed granites, metavolcano-sedimentary successions, and metavolcanic successions. Based on Nd–Sr isotopic and U–Pb geochronological data, Cordani et al. (2010a) demonstrate that the RACT is composed of two major terranes with distinct evolutionary histories (Western and Eastern Terranes). We recognized a third terrane, defined as the Southeastern Terrane (Fig. 2). The Western and Eastern Terranes are separated by the Aldeia Tomázia shear zone, a top-to-west low-angle thrust zone responsible for placing slightly deformed lower greenschist facies rocks (Western Terrane) and highly deformed amphibolite facies rocks (Eastern Terrane) side by side. The Eastern and Southeastern Terranes present the same metamorphic and deformational patterns and are separated by the Serra do Perdido dextral strike-slip shear zone (Fig. 2). A mafic dyke swarm (Rio Perdido Suite; Lima et al., 2012) intruded all of the units of the RACT. There are no geochronological data for this dyke swarm. However, although undeformed, part of the dyke swarm was metamorphosed, suggesting a minimal age of ca. 1300 Ma (^{40}Ar – ^{39}Ar data of Cordani et al., 2010a, 2010b, obtained on regionally metamorphosed units, Fig. 2).

2.1. Western Terrane

The Western Terrane is composed of gneissic and granitic rocks of the Porto Murtinho Complex, which was intruded by granitic rocks of the Chatelodo Granite and the Alumiador Suite and recovered by volcanic and pyroclastic rocks of the Serra da Bocaina Formation (Cordani et al., 2010a). We recognize two units related to the Porto Murtinho Complex: Córrego Jibóia Gneiss (gray mylonitic orthogneiss of monzogranitic protolith) and Morro da Lenha Granite (undeformed green porphyritic monzogranite) (Fig. 2). No geochronological data are available for the Porto Murtinho Complex, but a minimum Orosirian age is indicated by the crystallization age of the Alumiador Suite (zircon U–Pb SHRIMP age of 1839 ± 33 Ma; Cordani et al., 2010a, 2010b) and of the volcanic rocks of the Serra da Bocaina Formation (zircon Pb–evaporation age of 1877 ± 4 Ma; Brittes et al., 2013). The Morro do Triunfo Gabbro is composed of dark-gray, medium-grained olivine gabbro, of which there are no data indicative of the crystallization age.

The Alumiador Suite comprises a series of undeformed to slightly deformed granitic plutons (Fig. 2) inferred to be part of an Orosirian magmatic arc (Lacerda Filho et al., 2006; Cordani et al., 2010a, 2010b). The most expressive and best studied pluton is the Alumiador Granite, a batholith with ellipsoidal shape (72 km-long and 20 km-wide), N–S orientation and approximately 800 km² of outcropping area. The Alumiador Granite is primarily composed of inequigranular hornblende-biotite monzogranite with a high-K calc-alkaline signature (Lacerda Filho et al., 2006; Manzano et al., 2012; Manzano, 2013) and a zircon U–Pb SHRIMP age of 1839 ± 33 Ma (Cordani et al., 2010a). Recent geological mapping and geochemical analyses indicate plutons with distinct petrological characteristics, including syncollisional signatures (Manzano et al., 2012; Manzano, 2013) and alkaline signatures of extensional settings (Pinto-Azevedo et al., 2014). The Alumiador Suite presents an average Nd T_{DM} model age of 2.52 Ga and an $\epsilon_{Nd(t)}$ between -5.91 and -2.86 , suggesting the presence of reworked crustal material to the magma source (Cordani et al., 2010a).

The Serra da Bocaina Formation is composed of acid and subordinate intermediate volcanic rocks classified as rhyolite and andesite, with a medium- to high-K calc-alkaline geochemical signature of volcanic arc settings (Godoy et al., 2010; Brittes et al., 2013). Many authors consider the Serra da Bocaina Formation to be the volcanic equivalent of the Alumiador Suite (e.g., Godoi et al., 2001; Lacerda Filho et al., 2006; Godoy et al., 2009, 2010; Manzano et al., 2012), an event named the Amoguijá Magmatic Arc (Lacerda Filho et al., 2006). Nevertheless, the available geochronological data (Cordani et al., 2010a, 2010b; Brittes et al., 2013) indicate that the Serra da Bocaina Formation is at least 40 Ma older than the Alumiador Granite and, thus, could not have been its volcanic equivalent.

The rocks of the Porto Murtinho Complex and the Alumiador Suite are partially covered by a meta-volcano-sedimentary succession named the Rio Naitaca Formation (Faleiros et al., 2013). Previously, this unit belonged to the Alto Tererê Formation (Cordani et al., 2010a, 2010b; Remédio et al., 2014). We propose restricting the Alto Tererê Formation to the supracrustal rocks that cover the Eastern and Southeastern Terranes. The Rio Naitaca Formation is composed of low-grade siliciclastic metasedimentary rocks, including meta-sandstone, meta-arkose, meta-wacke, slate and phyllite, and subordinate metavolcanic and pyroclastic rocks. The Rio Naitaca Formation is regionally metamorphosed under lower greenschist facies conditions (chlorite zone), locally reaching middle greenschist facies conditions (biotite zone). The observed contact relationships with the rocks of the Porto Murtinho Complex are of a tectonic nature.

2.2. Eastern Terrane

The Eastern Terrane is composed of mylonitic orthogneisses (Morraria Gneiss and Caracol Gneiss) and undeformed to slightly deformed granites of the Baía das Garças Suite (Cordani et al., 2010a). The Morraria Gneiss is composed of gray banded gneiss with common intercalations of amphibolite lenses. The Morraria Gneiss has a zircon U–Pb SHRIMP age of 1950 ± 23 Ma (Cordani et al., 2010a). The Caracol Gneiss comprises pinkish leucocratic granitic gneisses with a zircon U–Pb SHRIMP age of 1774 ± 26 Ma (Cordani et al., 2010a). Major and trace element whole-rock geochemical analyses obtained in rocks from the Morraria and Caracol Gneisses indicate subduction-related calc-alkaline signatures (Lacerda Filho et al., 2006). However, whole-rock geochemical analyses (major and trace elements) obtained by Remédio et al. (2014) on rocks of the Caracol Gneiss are dominated by evolved alkaline signatures of extensional settings (Type A-like affinity). Samples of the Caracol Gneiss exhibit Nd T_{DM} model ages between 1.97 and 2.23 Ga and $\epsilon_{Nd(t)}$ from -1.94 to $+0.97$, suggesting juvenile magma sources with some contribution of reworked crustal material (Cordani et al., 2010a).

The Baía das Garças Suite presents zircon U–Pb SHRIMP ages of 1754 ± 49 Ma and 1721 ± 25 Ma, an average Nd T_{DM} model age of 2.02 Ga and a slightly positive $\epsilon_{Nd(t)}$, suggesting that juvenile sources were dominant for the magmatism (Cordani et al., 2010a). Major and trace element geochemical data available for the Sanga Bonita, Espinilho and Santa Clarinha plutons (Fig. 2), correlated to the Baía das Garças Suite, indicate subduction-related, high-K, calc-alkaline signatures (Remédio et al., 2014). The Cerro Porã Granite is an elongated pluton occurring at the southwestern margin of the Eastern Terrane, which presents alkaline geochemical signatures of extensional settings and a zircon U–Pb SHRIMP age of 1749 ± 45 Ma (Plens et al., 2013).

2.3. Southeastern Terrane

The Southeastern Terrane is composed of two granitic units (Rio da Areia Augen Gneiss and Scardine Granite) that intruded a banded biotite gneiss of monzogranitic composition (Remédio et al., 2014), named here the João Cândido Gneiss. The Rio da Areia Augen Gneiss was intensely deformed during a regional tectono-metamorphic event, while the Scardine Granite was only locally deformed during the same event. Geochemical analyses carried out in rocks from the João Cândido Gneiss indicate coexisting signatures of the high-K calc-alkaline and alkaline series, suggesting a post-collisional to anorogenic environment (Remédio et al., 2014). The Rio da Areia Augen Gneiss is dominated by porphyroclastic mylonitic monzogranite with a geochemical signature of syncollisional high-K calc-alkaline magma series, while the Scardine Granite is dominated by undeformed coarse- to medium-grained equigranular granite with a geochemical signature of the alkaline series of extensional settings (Remédio et al., 2014).

2.4. Alto Tererê Formation

The Alto Tererê Formation is a supracrustal rock unit that partially covers the Western, Eastern and Southeastern Terranes (Fig. 2). It is dominated by medium-grade siliciclastic metasedimentary rocks, including garnet quartzite, feldspathic quartzite and garnet-mica schist, with subordinate lenses of amphibolite. The stratigraphic position of the Alto Tererê Formation has been a matter of debate due to ambiguous contact relationships with adjacent units, with extensive overprinting by intense shearing. The unit was inferred as a sedimentary cover of basement gneisses and granites based on the apparent stratigraphic stacking (Corrêa et al., 1976; Nogueira et al., 1978; Correia Filho et al., 1981; Godoi et al., 2001) or as the oldest unit of the RACT (Lacerda Filho et al., 2006). Lacerda Filho et al. (2014) present a zircon U–Pb age of 1768 ± 6 Ma for a basal amphibolite from the Alto Tererê Formation and minimum detrital zircon U–Pb ages at approximately 1700 Ma for siliciclastic units. These data indicate that the siliciclastic units of the Alto Tererê Formation are younger than the granitic and gneissic basement of the RACT.

The Alto Tererê Formation records a Barrovian-type metamorphism, varying from upper greenschist facies (garnet zone) to middle amphibolite facies conditions (kyanite zone), with an age between 1310 and 1270 Ma (^{40}Ar – ^{39}Ar and K–Ar data of Araújo et al., 1982; Cordani et al., 2010a,b; monazite U–Pb data of Lacerda Filho et al., 2014).

3. Analytical methods

We selected 14 samples of key geological units of the RACT for zircon U–Pb geochronology. U–Pb geochronological determinations were obtained from zircon grains extracted from individual samples using common procedures involving crushing, disk-milling and separation using standard heavy liquid and magnetic techniques. Afterward, zircon grains were hand-picked, selected, mounted in epoxy and polished. U–Pb determinations were performed by SHRIMP at the Geochronology Research Center of the University of São Paulo (CPGeo-USP) and by LA-MC-ICP-MS at the Isotope Geology Laboratory of the Geosciences Institute of the Federal University of Rio Grande do Sul (UFRGS) and the Laboratory of Geochronology at the University of Brasília (UnB).

Zircon grains analyzed by SHRIMP were mounted together with the TEMORA standard and coated with Au after polishing. Cathodoluminescence (CL) images of the polished mounts were obtained using a FEI-QUANTA 250 FEG scanning electron microscope equipped with a Centaurus Mono CL3 + cathodoluminescence spectroscope at the CPGeo-USP. The mounts were then analyzed by U–Pb isotopic technique using a SHRIMP-IIe machine at the CPGeo-USP, following analytical procedures described in Williams (1998). Correction for common Pb was made based on the ^{204}Pb measured, and the typical error component for the $^{206}\text{Pb}/^{238}\text{U}$ ratio is less than 2%. The U abundance and U–Pb ratios were calibrated against the TEMORA standard.

Backscattered electron (BSE) images of zircons analyzed by LA-MC-ICP-MS were obtained using a JEOL JSM 5800 electron microscope (UFRGS) and an FEI Quanta 450 scanning electron microscope (UnB). LA-MC-ICP-MS isotopic analyses were performed using Finnigan Neptune instruments coupled to ablation systems with a Nd-YAG laser ($k = 213$ nm) from the New Wave Research at UFRGS and UnB. The grains were ablated at a spot size of 30 μm , a frequency of 10 Hz and an intensity between 0.19 and 1.02 J/cm². The pulverized material was transported by a flow of He (~0.40 L/min) and Ar (~0.90 L/min) in analyses of 40 cycles of 1 s. The international standard GJ-1 was used to correct the drift of the equipment as well as the fractionation between the U and Pb isotopes. The standards UQZ (UFRGS) and TEMORA-2 (UnB) were used to verify the accuracy of the analyses. The data collection procedure followed the reading sequence: 1 blank, 1 standard, 4 samples, 1 blank and 1 standard. Each reading determined

Table 1

Description and location of samples with zircon U–Pb analyses performed in this work. Abbreviations for deformation mechanisms: GBM: grain boundary migration recrystallization, BLG: bulging recrystallization.

Sample	Unit	Lithology	Mineralogy		Deformation mechanism		Age (Ma)	Method	Latitude	Longitude	Terrane
			Primary	Metamorphic	Quartz	Feldspar					
FM-101A	Córrego Jibóia Gneiss (Porto Murтинho Complex)	Mylonitic granitic gneiss	Mc, Qtz, pseudomorphs of Pl and Bt, Ttn, Ap, Zrn	Se, Ep, Ab (35 vol.%)	GBM superposed by BLG	BLG	1947 ± 9 (1989 ± 11 inheritance)	SHRIMP	−20.49830	−57.25810	Western
FM-128A	Morro da Lenha Granite (Porto Murтинho Complex)	Hydrothermalized porphyritic biotite monzogranite	Mc, Qtz, pseudomorphs of Pl and Bt, Zrn	Se, Ep, Bt, Ap, Ab, Cb (55 vol.%)	Very weak intracrystalline deformation	No ductile deformation	1941 ± 13	SHRIMP	−20.83890	−57.34790	Western
MS-141A	Chatelodo Granite	Granophyric syenogranite	Pl, Kfs, Mag, Bt	Ep, Se, Chl, Ttn, Opq	Very weak intracrystalline deformation	No ductile deformation	1902 ± 12	SHRIMP	−21.45277	−57.46107	Western
MS-110B	Porto Murтинho Gneiss (Porto Murтинho Complex)	Retrometamorphosed gneiss		Chl, Se, Ep, Ab, Qtz, Rt, Opq, Zrn, Mnz, pseudomorphs of Pl and Kfs	SGR superposed by BLG		1910–1950	SHRIMP	−21.19436	−57.39275	Western
MS-29A	Córrego do Ceruo Granite (Alumiador Suite)	Granophyric syenogranite	Mc, Pl, Qtz, Bt, Mag, Grt, Ttn, Zrn	Se, Chl, Ep, Fl	BLG	No ductile deformation	1841 ± 15	SHRIMP	−21.34595	−57.10801	Western
FM-57	Santa Otilia Granite (Alumiador Suite)	Granophyric syenogranite	Pl, Mc, Qtz, Mag, Ttn, Zrn	Se, Ep, Bt	No ductile deformation	No ductile deformation	1830 ± 12	SHRIMP	−20.97440	−57.29890	Western
VC-15	Rio da Areia Augengneiss	Porphyroclastic biotite monzogranite	Mc, Qtz, Pl, Bt, Mag, Ttn, Ap, Zrn	Ep, Se, Chl, Ab	GBM	BLG	1809 ± 9	LA-MC-ICP-MS	−21.97719	−56.84445	Southeastern
FM-169A	Rio Naitaca Formation	Andesitic lapilli tuff	Pl, Qtz	Chl, Ep, Cb	No ductile deformation	No ductile deformation	1813 ± 18	SHRIMP	−20.60150	−57.47930	Western
MR-159	Scardine Granite	Hornblende-biotite monzogranite	Qtz, Pl, Mc, Bt, Hbl, Ap, Zrn	Ep	No ductile deformation	No ductile deformation	1791 ± 19	LA-MC-ICP-MS	−21.68059	−56.89012	Southeastern
MS-50A	Caracol Gneiss	Biotite granodiorite	Pl, Qtz, Mc, Bt, Zrn, Rt, Ttn, Opq	Ep, Ms, Chl	GBM	Intracrystalline deformation	1781 ± 7	LA-MC-ICP-MS	−21.431	−57.019	Eastern
FM-147	Caracol Gneiss	Syenogranitic muscovite-biotite gneiss	Mc, Qtz, Pl, Bt, Mag, Ttn, Zrn	Ms, Ep, Cb	GBM	Intracrystalline deformation	1753 ± 13	SHRIMP	−20.84290	−57.06490	Eastern
MR-50	Santa Clarinha Orthogneiss (Baia das Garças Suite)	Monzogranitic hornblende-biotite gneiss	Mc, Qtz, Pl, Bt, Hbl, Ttn, Ap, Zrn	Ep, Se, Chl	Intracrystalline deformation	No ductile deformation	1750 ± 9	LA-MC-ICP-MS	−21.54568	−56.92784	Eastern
VC-83A	Espinilho Orthogneiss (Baia das Garças Suite)	Monzogranitic biotite gneiss	Qtz, Mc, Pl, Bt, Mag, Zrn	Py, Chl, Se, Ep	Intracrystalline deformation	No ductile deformation	1719 ± 11	LA-MC-ICP-MS	−21.60155	−56.96713	Eastern
FM-173	Rio Perdido Suite	Microgabbonorite	Opx, Cpx, Pl, Zrn	Ep, Se, Act, Bt	No deformation	No deformation	1589 ± 44	LA-MC-ICP-MS	−20.624	−57.469	Western

398 the intensities of the masses of ^{202}Hg , $^{204}(\text{Pb} + \text{Hg})$, ^{206}Pb , ^{207}Pb , ^{208}Pb
 399 and ^{238}U . The reduction of the raw data followed the procedure
 400 described in Bühn et al. (2009).

401 SHRIMP and LA-MC-ICP-MS ages were calculated using the ISOPLOT
 402 3.0 program (Ludwig, 2003).

403 4. Results

404 A summary with descriptions of analyzed samples and zircon U–Pb
 405 ages is presented in Table 1, while detailed petrographic descriptions
 406 are presented in the Supplementary material. Locations of the analyzed
 407 samples are displayed in Fig. 2.

4.1. Western Terrane

4.1.1. Córrego Jibóia Gneiss (Porto Murinho Complex)

409 The Córrego Jibóia Gneiss (Faleiros et al., 2014) outcrops as a series
 410 of isolated small hills over a wide area covered by Quaternary sediments
 411 of the Pantanal Formation (Fig. 2). Sample FM-101A is a gray proto-
 412 mylonitic monzogranite with an igneous inequigranular seriated tex-
 413 ture largely preserved despite the superposed deformation. Secondary
 414 sericite, epidote and albite represent approximately 35 vol.% of the
 415 rock. The sample presents euhedral to subhedral zircon grains with
 416 sizes between 60 and 205 μm and an aspect ratio from 1:1 to 4:1. CL
 417 images indicate two populations of zircons, one composed of dark crystals
 418 (higher U contents) with oscillatory zoning and the other composed
 419



Fig. 3. Cathodoluminescence images showing the zircon grains analyzed by U–Pb SHRIMP isotopic technique. Black and white circles indicate the location of the performed spot analyses. Numbers in the bottom left corners are sample numbers discussed in the text.

of grains with light cores (lower U contents) and dark rims, both with oscillatory zoning (Fig. 3a). Fifteen SHRIMP analyses were performed in the cores and rims of the zircon grains (Table S1, Supplementary

data), but three analyses were discarded due to high analytical errors; the remaining analyses are concordant within analytical errors. The internal structure of zircon grains in conjunction with spot U–Pb data

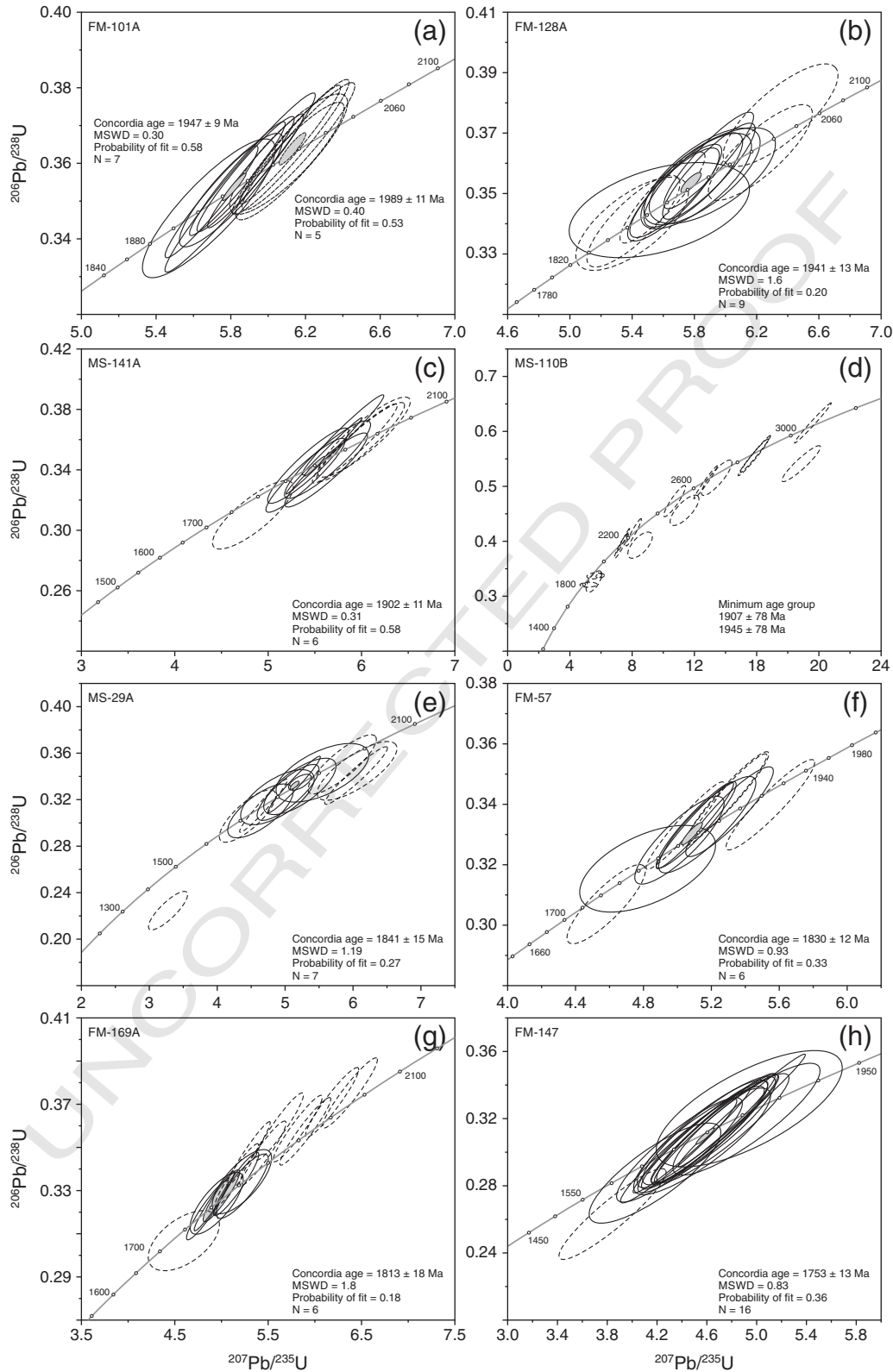


Fig. 4. Concordia diagrams showing the analytical points of the U–Pb SHRIMP zircon analyses of rocks from the Rio Apa Cratonic Terrane. Numbers in the top left corners are sample numbers discussed in the text. Solid and dashed line ellipses represent data used and not used in the calculations of concordia ages, respectively. Ages and error ellipses are stated to 2σ (95%) confidence limits.

allow us to interpret two age populations: (1) five analyses performed on low-U zircon cores (light in CL images) yield a concordia age of 1989 ± 11 Ma (mean square of the weighted deviates = MSWD = 0.40; Fig. 4a), which we interpret as inheritance; and (2) seven analyses carried out on high-U zircon rims and homogeneous grains (dark in CL images) yield a concordia age of 1947 ± 9 Ma (MSWD = 0.30; Fig. 4a), inferred as a magmatic crystallization age.

4.1.2. Morro da Lenha Granite (Porto Murtinho Complex)

The Morro da Lenha Granite (Faleiros et al., 2014) is an ellipsoidal stock that outcrops over 7.2 km², displaying an aspect ratio of 1:8 with a NW-trending orientation (Fig. 2). Its margins are covered by sediments of the Pantanal Formation. Sample FM-128A, representative of the main lithotype of the pluton, is a dark green hydrothermalized porphyritic monzogranite with phenocrysts of pinkish microcline in a medium- to coarse-grained matrix. The sample presents euhedral to subhedral prismatic zircon grains with a size in the range of 65 to 290 μm, an aspect ratio between 2:1 and 7:1 and oscillatory compositional zoning (Fig. 3b). Some grains present irregularly shaped cores truncated by rims with oscillatory zoning (Fig. 3b). Fifteen SHRIMP analyses were performed in zircon grains (Table S1), of which 14 analyses are concordant, within analytical errors. Nine spot analyses are distributed in a central cluster in the Concordia diagram and yield a concordia age of 1941 ± 13 Ma (MSWD = 1.6; Fig. 4b). The remaining spot analyses are distributed in two marginal clusters at ages of approximately 1890 and 2010 Ma (Fig. 4b). However, the internal structures and isotopic composition of the analyzed zircon grains do not allow us to establish the existence of zircon zones or grains with different crystallization ages with certainty. In fact, this pattern could be a result of isotopic disequilibrium. Thus, we interpret the age of 1941 ± 13 Ma as the most representative crystallization age for the Morro da Lenha Granite.

4.1.3. Chatelodo Granite

The Chatelodo Granite (Pavan et al., 2014) occurs as a series of small outcrops (2 × 5 m wide) along the western part of the study area. It is partially covered by metavolcanic rocks from the Serra da Bocaina Formation (Pb-evaporation age of 1877 ± 4 Ma; Brittes et al., 2013) and by sediments of the Pantanal Formation. Sample MS-141A is a hololeucocratic pinkish to greenish porphyritic syenogranite, with plagioclase and alkali feldspar phenocrysts set in a fine- to medium-grained matrix. The sample presents one population of prismatic zircon grains with an aspect ratio of 2:1 and slightly rounded terminations. The CL images show grains with dark and light cores and rims presenting regular to irregular compositional zoning (Fig. 3c). Fifteen SHRIMP analyses were performed (Table S1), of which ten analyses are concordant, within analytical errors. Five analyses were discarded due to high common Pb. The data are distributed along a main central age cluster with six concordant analyses yielding a concordia age of 1902 ± 11 Ma (MSWD = 0.31; Fig. 4c), interpreted as the best estimate for the time of crystallization of the pluton. The three remaining analyses have an apparent age of ~1970 Ma, but there is no textural or compositional evidence to interpret this age as geologically significant; thus, it can represent an isotopic disequilibrium.

4.1.4. Porto Murtinho Gneiss (Porto Murtinho Complex)

The dominant lithological unit of the Porto Murtinho Complex occurs on the western portion of the study area (Fig. 2). Sample MS-110B is a retrometamorphic gray banded gneiss typical of this unit, and it presents a greenschist facies assemblage (chlorite + sericite ± albite) that corresponds to approximately 60 vol.% of the rock. The sample presents zircon grains with rounded terminations and regular and irregular compositional zoning, and some grains show inherited cores and newer rims (Fig. 3d). Sixteen SHRIMP analyses were performed (Table S1). Twelve of these are concordant, within analytical errors, and they span the age interval from 1900 to 3200 Ma (Fig. 4d).

The morphology of the zircon grains is characteristic of detrital grains, and the ages must be interpreted as source ages. We interpret the youngest age group (1900–1950 Ma) as the maximum depositional age for the sample.

4.1.5. Córrego do Cervo Granite (Alumizador Suite)

The Córrego do Cervo Granite (Pavan et al., 2014) is an elongated batholith of approximately 270 km² of outcropping area and N–S-trending orientation (Fig. 2). Its boundaries are defined by mylonitic zones in contact with rocks from the Alto Tererê Formation and the Caracol Gneiss. Sample MS-29A is a pinkish protomylonitic syenogranite, with a fine- to medium-grained seriated and granophyric texture. The sample presents one population of prismatic zircons with a grain size from 65 to 200 μm, an aspect ratio between 2:1 and 3:1 and rounded terminations. The CL images show grains with predominantly dark cores and regular to irregular compositional zoning (Fig. 3e). Thirteen SHRIMP spot analyses were performed in zircon grains (Table S1), including cores and rims. The data are distributed along a main central age cluster with seven concordant analyses yielding a concordia age of 1841 ± 15 Ma (MSWD = 1.19; Fig. 4e). Three remaining analyses have apparent ages of ~1970 Ma, but there is no textural or compositional evidence to interpret this age as geologically significant. We interpret the age of 1841 ± 15 Ma as the time of pluton crystallization.

4.1.6. Santa Otilia Granite (Alumizador Suite)

The Santa Otilia Granite (Faleiros et al., 2014; Pavan et al., 2014) is an ellipsoidal batholith of 264 km² of outcropping area, an aspect ratio of 3:1 and a NNW-trending orientation (Fig. 2). It is partially in tectonic contact with rocks of the Alto Tererê Formation and partially covered by metasedimentary rocks of the Rio Naitaca Formation and sediments of the Pantanal Formation. Sample FM-57 is a medium-grained pinkish granophyre with an isotropic structure and syenogranitic composition and is representative of the main lithotype present in the batholith. The sample presents euhedral zircon grains with sizes from 50 to 100 μm and an aspect ratio between 1:1 and 2:1. The CL images show grains with oscillatory compositional zoning and no inherited cores (Fig. 3f). Fifteen SHRIMP spot analyses were performed in zircon grains (Fig. 3f, Table S1). All of the analyses are concordant within errors, but four analyses were discarded due to high content of common Pb. The data are distributed along a main central age cluster with six concordant analyses yielding a concordia age of 1830 ± 12 Ma (MSWD = 0.93; Fig. 4f), interpreted as the best estimate for the time of crystallization of the pluton.

4.1.7. Rio Naitaca Formation

The Rio Naitaca Formation (Fig. 2) is composed of very low-grade meta-arkose, meta-wacke, slate and phyllite, with common intercalations of layers of meta-andesitic volcanic rocks and pyroclastic rocks. Sample FM-169A comes from the base of the Rio Naitaca Formation and comprises a foliated dark-green pyroclastic rock that occurs intercalated with meta-sandstone layers. It is composed of approximately 70 vol.% of angular to sub-rounded lapilli to bomb fragments of andesite tuffs and approximately 30 vol.% of domains of feldspathic wackestone or arkose. The sample displays prismatic, rounded and fragmented zircon grains with sizes varying from 80 to 235 μm and aspect ratios between 1:1 and 7:1. The CL images show grains with regular and complex oscillatory zoning (Fig. 3g). Fifteen U–Pb SHRIMP analyses were performed on zircon grains (Table S1). Six concordant analyses of a youngest zircon group yield a concordia age of 1813 ± 18 Ma (MSWD = 1.8; Fig. 4g), interpreted as the time of crystallization of the andesite fragments and of the sedimentation of the base of the Rio Naitaca Formation. Four remaining concordant analyses yield ²⁰⁷Pb–²⁰⁶Pb ages from 1918 ± 11 Ma to 2003 ± 11 Ma (Table S1), interpreted as detrital zircon input.

4.2. Eastern Terrane

4.2.1. Caracol Gneiss

The Caracol Gneiss (Cordani et al., 2010a, 2010b) is dominated by pinkish, hololeucocratic, foliated granites with monzogranitic to syenogranitic composition. Sample MS-50A comes from a kilometer-scale body of granodioritic banded gneiss hosted by the main rocks of the Caracol Gneiss. The sample presents one population of subhedral to euhedral zircon with grain sizes from 160 to 600 μm and aspect ratios between 1:1 and 4:1. The BSE images show grains with weak oscillatory compositional zoning and no inherited cores (Fig. 5a). Twenty-one U–Pb LA-MC-ICP-MS analyses were performed (Table S1), including core and rim analyses, yielding an upper intercept age of 1781 ± 7 Ma (MSWD = 1.5) (Fig. 6a). This age is interpreted as the time of crystallization of the rock.

Sample FM-147 is a light gray gneiss of syenogranitic composition associated with regionally abundant, pinkish, foliated granites. The sample presents subhedral zircon grains with sizes varying from 100 to 250 μm , aspect ratios between 2:1 and 3:1, and complex compositional zoning, including domains with oscillatory zoning (Fig. 3h). Seventeen U–Pb SHRIMP analyses were performed (Table S1), of which 16 are concordant and yield a concordia age of 1753 ± 13 Ma (MSWD = 0.83; Fig. 4h), interpreted as the time of crystallization of the rock.

4.2.2. Santa Clarinha Orthogneiss

The Santa Clarinha Orthogneiss (Remédio et al., 2013) is an ellipsoidal body with an aspect ratio of 6:1, a NE-trending orientation and approximately 450 km^2 of outcropping area (Fig. 2), which we interpret as associated with the Baía das Garças Suite. Sample MR-50 is a monzogranitic gneiss with a foliation defined by the preferred orientation of millimeter-thick mafic lenses composed of biotite, epidote, hornblende and titanite. The sample presents prismatic zircon grains with rounded terminations and an aspect ratio between 1:1 and 3:1. The BSE images show grains primarily of homogeneous composition. Twenty-five LA-MC-ICP-MS analyses were performed (Table S1), including core and rim analyses, but five analyses were discarded due to elevated analytical errors. The remaining analyses are concordant, but they show a relatively large scattering on the concordia around a central age. Thirteen concordant analyses yield an upper intercept age of 1742 ± 10 Ma (MSWD = 0.93) (Fig. 6b). Eight analyses yield a concordia age of 1750 ± 9 Ma (MSWD = 0.48) (Fig. 6b), interpreted as the best estimate for the time of crystallization of the Santa Clarinha Orthogneiss.

4.2.3. Espinilho Orthogneiss

The Espinilho Orthogneiss (Remédio et al., 2013) comprises a deformed granitic stock with ellipsoidal shape (aspect ratio of 1.6), a

NW-trending orientation and an outcropping area of approximately 0.7 km^2 . Sample VC-83A is a light-brown, medium-grained, equigranular biotite-gneiss of monzogranitic composition. The sample exhibits two zircon populations, both with an aspect ratio between 1:1 and 2:1. One population is composed of rounded grains, while the other is composed of prismatic grains with rounded terminations. The BSE images show the internal compositional zoning characteristic of igneous zircons, without inherited cores. Twenty-three LA-MC-ICP-MS analyses were performed (Table S1), including core and rim analyses. Nevertheless, there is no significant variation of ages between the different zones. The 23 spot analyses yield an upper intercept age of 1713 ± 14 Ma (MSWD = 1.09) (Fig. 6c), with a lower intercept toward the Neoproterozoic, but with large errors. Thirteen analyses define a concordia age of 1719 ± 11 Ma (MSWD = 0.26) (Fig. 6c), interpreted as the best estimate for the time of crystallization of the Espinilho Orthogneiss.

4.3. Southeastern Terrane

4.3.1. Rio da Areia Augen Gneiss

The Rio da Areia Augen Gneiss (Remédio et al., 2013) is a deformed batholith elongated along the N–S direction (Fig. 2), with approximately 350 km^2 of outcropping area. Its eastern portion is unconformably overlain by undeformed Ediacaran siliciclastic sedimentary rocks from the Corumbá Group. Its western portion is in tectonic contact with rocks from the Caracol Gneiss and the Sanga Bonita Granite. The Rio da Areia Augen Gneiss is composed of heterogeneously mylonitized porphyritic granitic rocks and subordinately mylonitic banded gneiss. Sample VC-15 is a reddish brown blastoporphyritic mylonitic gneiss of monzogranitic composition. The sample presents prismatic zircon grains with rounded terminations and an aspect ratio between 2:1 and 3:1. The BSE images show a dominance of grains with regular and irregular compositional zoning and uncommon grains with a homogeneous composition. Twenty LA-MC-ICP-MS spot analyses were completed (Table S1), of which 17 yield an upper intercept age of 1820 ± 18 Ma (MSWD = 4.7) (Fig. 6d). A sole concordant analysis yields an age of 1809 ± 9 Ma (Fig. 6d), which we interpret as the best estimate for the time of crystallization of the pluton.

4.3.2. Scardine Granite

The Scardine Granite (Remédio et al., 2013) is a semi-circular pluton of approximately 91 km^2 of outcropping area that intruded banded rocks from the João Cândido Gneiss (Fig. 2). Both the granite and its host rocks are unconformably overlain in part by siliciclastic sedimentary rocks of the Corumbá Group. Sample MR-159 comprises a medium-grained equigranular pinkish monzogranite with isotropic structure. The sample displays only one zircon population consisting of prismatic grains with an aspect ratio of approximately 2:1. The BSE images

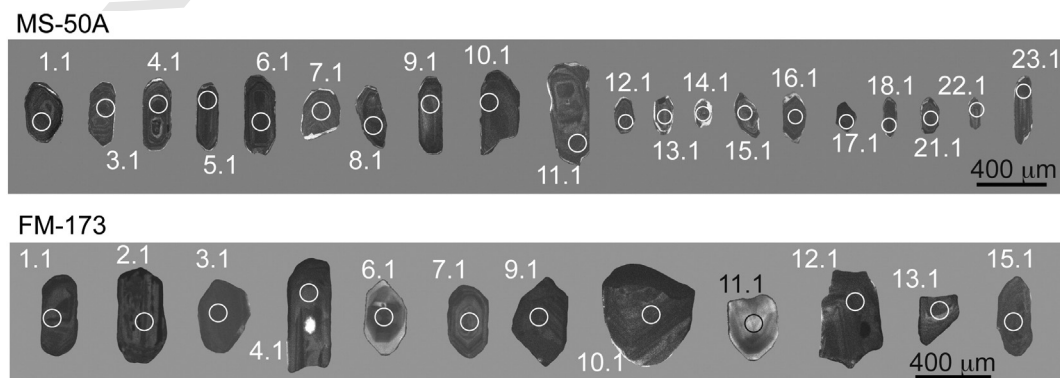


Fig. 5. Back-scattered electron images showing the zircon grains analyzed by U–Pb LA-MC-ICP-MS isotopic technique. Black and white circles indicate the location of the performed spot analyses. Numbers in bottom left corners are sample numbers discussed in the text.

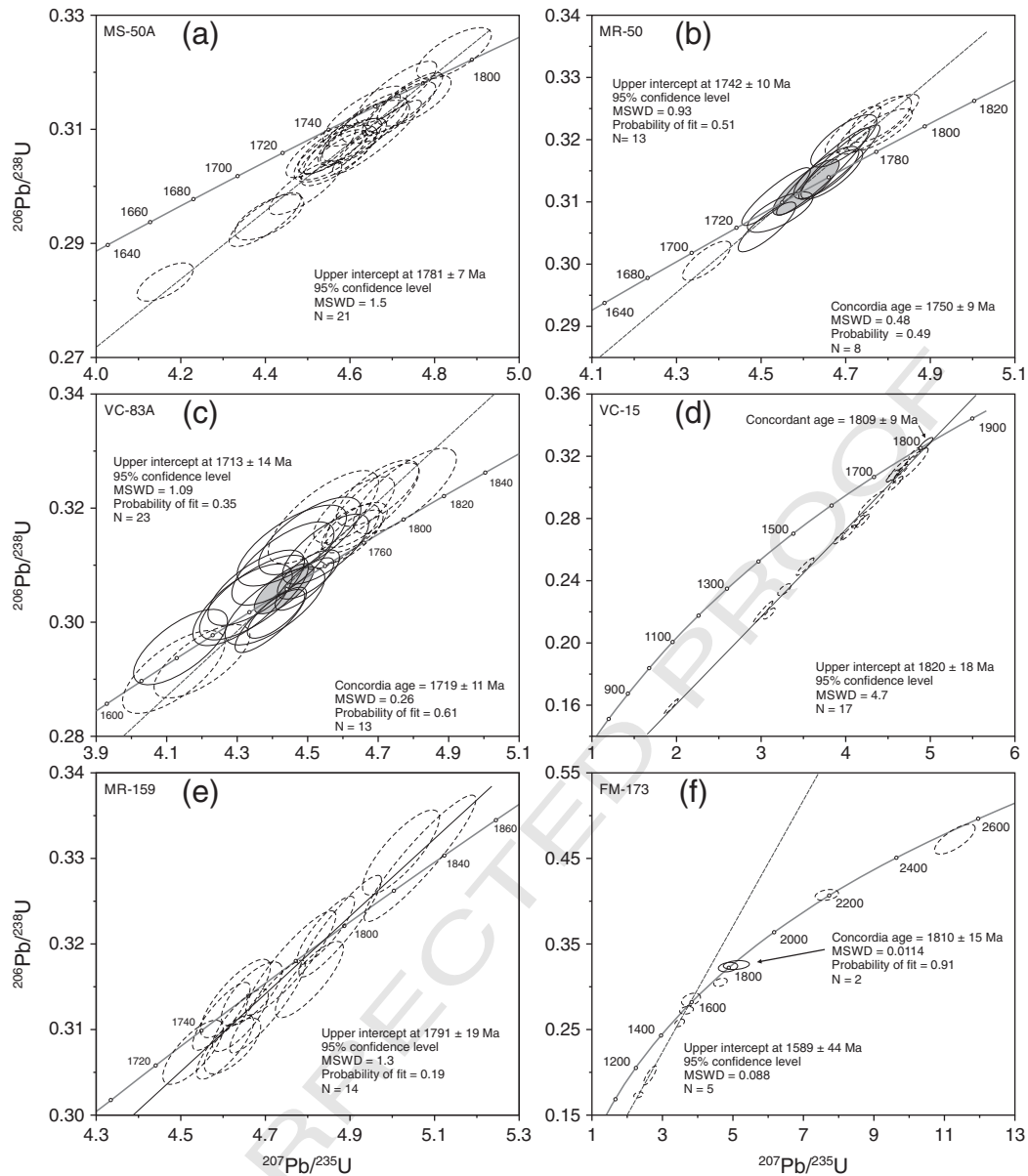


Fig. 6. Concordia diagrams showing the analytical points of the U–Pb LA-MC-ICP-MS zircon analyses of rocks from the Rio Apa Cratonic Terrane. Numbers in top left corners are sample numbers discussed in the text. Solid and dashed line ellipses represent data used and not used in the calculations of concordia ages, respectively. Ages and error ellipses are stated to 2σ (95%) confidence limits.

show that compositionally homogeneous grains are dominant. Twenty-six LA-MC-ICP-MS analyses were performed (Table S1), 14 of which, with 97 to 102% of concordance, define an upper intercept age of 1791 ± 19 Ma (MSWD = 1.3) (Fig. 6e), interpreted as the time of crystallization of the Scardine Granite.

4.4. Rio Perdido Suite

Sample FM-173 is a dark-gray isotropic microgabbro collected from an E–W-trending subvertical dyke of the Rio Perdido Suite. The dyke is hosted by rocks from the Rio Naitaca Formation in the Western Terrane. The sample presents rounded, anhedral and prismatic zircon grains (Fig. 5b). The BSE images show the coexistence of homogeneous grains and grains with oscillatory and complex compositional zoning (Fig. 5b). Fifteen U–Pb LA-MC-ICP-MS analyses were performed (Table S1), but five analyses were discarded due to elevated analytical error. Five analyses with the youngest apparent ages define an upper

intercept age of 1589 ± 44 Ma (MSWD = 0.088; Fig. 6f), interpreted as the time of the dyke crystallization. The five remaining analyses present apparent ^{207}Pb – ^{206}Pb ages of approximately 1800, 2200 and 2600 Ma (Fig. 6f; Table S1), which we interpret as detrital zircon xenocrysts. Two concordant analyses of the youngest xenocrysts yield a concordia age of 1810 ± 15 Ma (MSWD = 0.0114; Fig. 6f), which coincides with the age of 1813 ± 19 Ma obtained for the host unit (sample FM-169A, Rio Naitaca Formation).

5. Discussion

The zircon U–Pb SHRIMP and LA-MC-ICP-MS data obtained in this work contribute to the chronostratigraphy of magmatism and the tectono-metamorphic events of the RACT, for which few high-quality age data exist. Table 2 gathers 22 available zircon U–Pb data, including 14 data from this work and eight published by Corđani et al. (2010a), Plens et al. (2013) and Brittes et al. (2013). The integration of the new

Table 2
 Summary of zircon U–Pb data available for the Rio Apa Cratonic Terrane. Geochemical signature interpretations are from Silva (1998), Lacerda Filho et al. (2006), Manzano et al. (2012), Brittes et al. (2013), Manzano et al., 2013, Plens et al. (2013), Faleiros et al. (2014), Pavan et al. (2014), Pavan and Faleiros (2014) and Remédio and Faleiros (2014).

Unit	Lithology	Age (Ma)	Chemical signature	Tectonic inferences	Terrane
Córrego Jibóia Gneiss (Porto Murinho Complex)	Mylonitic granitic gneiss	1989 ± 11 ^a		Inheritance	Western
Córrego Jibóia Gneiss (Porto Murinho Complex)	Mylonitic granitic gneiss	1947 ± 9 ^a	Calc-alkaline	Arc-related plutonism	Western
Morraria Gneiss	Migmatitic banded gneiss	1950 ± 23 ^c		Arc-related plutonism	Eastern
Morro da Lenha Granite (Porto Murinho Complex)	Porphyritic biotite monzogranite	1941 ± 13 ^a	Calc-alkaline	Arc-related plutonism	Western
Chatelodo Granite	Granophyric syenogranite	1902 ± 12 ^a	High-K calc-alkaline	Arc-related plutonism	Western
Porto Murinho Gneiss (Porto Murinho Complex)	Retrometamorphosed gneiss	1910–1950 ^a		Maximum depositional age	Western
Serra da Bocaina Formation	Ignimbrite	1877 ± 4 ^d	Medium- to high-K calc-alkaline	Arc-related volcanism	Western
Córrego do Cervo Granite (Alumiador Suite)	Granophyric syenogranite	1841 ± 15 ^a	Alkaline (Type A-like)	Post-collisional magmatism	Western
Alumiador Granite (Alumiador Suite)	Porphyritic hornblende-biotite monzogranite	1839 ± 33 ^c	High-K calc-alkaline	Arc-related plutonism	Western
Santa Otilia Granite (Alumiador Suite)	Granophyric syenogranite	1830 ± 12 ^a	Alkaline (Type A-like)	Post-collisional magmatism	Western
Rio da Areia Augengneiss	Porphyroclastic biotite monzogranite	1809 ± 9 ^b	High-K calc-alkaline	Syncollisional magmatism	Southeastern
Rio Naitaca Formation	Andesitic lapilli tuff	1813 ± 18 ^a	Medium-K tholeiitic	Arc-related volcanism	Western
Scardine Granite	Hornblende-biotite monzogranite	1791 ± 19 ^b	Alkaline (Type A-like)	Post-collisional magmatism	Southeastern
Caracol Gneiss	Biotite granodiorite	1781 ± 7 ^b	High-K calc-alkaline and alkaline	Granitic plutonism	Eastern
Caracol Gneiss	Leucogranite	1774 ± 26 ^c	High-K calc-alkaline and alkaline	Granitic plutonism	Eastern
Caracol Gneiss	Syenogranitic muscovite-biotite gneiss	1753 ± 13 ^a	High-K calc-alkaline and alkaline	Granitic plutonism	Eastern
Baia das Garças Granite (Baia das Garças Suite)	Granite	1754 ± 42 ^c	High-K calc-alkaline	Granitic plutonism	Eastern
Cerro Porã Granite (Baia das Garças Suite)	Granite	1749 ± 45 ^e	Alkaline (Type A-like)	Post-collisional magmatism	Eastern
Santa Clarinha Orthogneiss (Baia das Garças Suite)	Monzogranitic hornblende-biotite gneiss	1750 ± 9 ^b	High-K calc-alkaline	Arc-related plutonism	Eastern
Sanga Bonita Granite (Baia das Garças Suite)	Porphyritic biotite monzogranite	1721 ± 25 ^c	High-K calc-alkaline	Arc-related plutonism	Eastern
Espinilho Orthogneiss (Baia das Garças Suite)	Monzogranitic biotite gneiss	1719 ± 11 ^b	High-K calc-alkaline	Arc-related plutonism	Eastern
Rio Perdido Suite	Dyke of microgabbro	1589 ± 44 ^b	Tholeiitic basic	Back-arc basin magmatism	All the RACT

^a Zircon U–Pb SHRIMP ages (this work).

^b Zircon U–Pb LA-MC-ICP-MS ages (this work).

^c Zircon U–Pb SHRIMP ages (Cordani et al., 2010a, 2010b).

^d Zircon Pb–evaporation ages (Brittes et al., 2013).

^e Zircon U–Pb SHRIMP ages (Plens et al., 2013).

U–Pb ages presented in this work with published U–Pb and geochemical data allows a great refinement and advance in understanding the tectonic evolution of the RACT, as summarized in Fig. 7.

The RACT is composed of smaller terranes with distinct evolutionary histories. Cordani et al. (2010a) recognized two distinct terranes (Eastern and Western Terranes) based on Sm–Nd model ages, and we recognized a third terrane, defined as the Southeastern Terrane. We will first discuss the evolutionary history of each terrane separately and then discuss the history of the terrane collage.

The available geochronological data (Table 2) indicate that the Western Terrane is made up of a granite–gneissic basement formed within the age interval of 1940–1950 Ma. The western portion of the Western Terrane was intruded by undeformed granites at approximately 1900 Ma (Chatelodo Granite) and was recovered by volcanic rocks at approximately 1880 Ma (Serra da Bocaina Formation). The granites of the Alumiador Suite, present throughout the Western Terrane, represent the next magmatic event, which occurred primarily between 1840 and 1830 Ma. These rocks were later overlain by immature sediments and associated synorogenic volcanic and pyroclastic rocks (Rio Naitaca Formation). A sample of lapilli-tuff from the base of the Rio Naitaca Formation indicates that deposition began at 1813 ± 19 Ma. Rocks from the Chatelodo Granite, Serra da Bocaina Formation and Alumiador Suite are largely undeformed, but the Alumiador Suite was intensely deformed at the contact zone with the Eastern Terrane. On the other hand, the Rio Naitaca Formation presents a progressive eastward increase of intensity in deformation and metamorphism. The whole deformational pattern of the Western Terrane indicates a dominant thin-skin deformation, where the basement was not involved in the deformation that affected the supracrustal rocks. An exception to this pattern is the highly deformed rocks from the Córrego Jibóia Gneiss (formed at ~1950 Ma), but the deformation of this unit could be related to an older event. Another important characteristic of the Western

Terrane is that the granitic plutons (Chatelodo Granite and Alumiador Suite) are dominated by subvolcanic rocks (e.g., granophyre), indicating a shallow-level crystallization pattern.

The Porto Murinho Gneiss, interpreted as a unit of sedimentary protolith, presented zircon ²⁰⁷Pb–²⁰⁶Pb ages spanning from 1900 to 3200 Ma, with a near continuous variation of ages throughout this interval (Fig. 4, Table S1). Detailed petrographic analysis of several samples from the Porto Murinho Gneiss has revealed that the whole unit underwent an intense lower greenschist facies metamorphic overprint, and the peak prograde metamorphism cannot be assessed (Pavan and Faleiros, 2014). The majority of the ages obtained from detrital zircons are significantly older than the ages of the gneissic and granitic units of the RACT, indicating that the main source rocks are not present in the RACT. Although there are insufficient data to define a robust maximum depositional age, the minimum age group (from 1907 ± 78 to 1945 ± 62 Ma) (Table S1) provides important constraints to possible geological correlations, indicating that the orthogneisses and granites from the Porto Murinho Complex might have contributed as source rocks. Intrusive contacts with the Alumiador Suite constrain a minimum depositional age of 1840–1830 Ma.

The available geochronological data (Table 2) indicate that the Eastern Terrane is primarily composed of granitic gneisses formed from 1780 to 1750 Ma (Caracol Gneiss) and intruded by granitic plutons in the period between 1750 and 1720 Ma (Baia das Garças Suite). Subsequently, this basement was covered by immature sedimentary deposits from the Alto Tererê Formation (maximum depositional age of ca. 1700 Ma; Lacerda Filho et al., 2014). Quartz and feldspar microstructures (Table 1; supplementary data) indicate that the rocks of the Caracol Gneiss and the Baia das Garças Suite underwent a regional moderate-temperature deformation phase (~500 °C) and a subsequent low-temperature deformation phase (300–400 °C), both associated with westward low-angle thrusting (Remédio and Faleiros, 2014). The

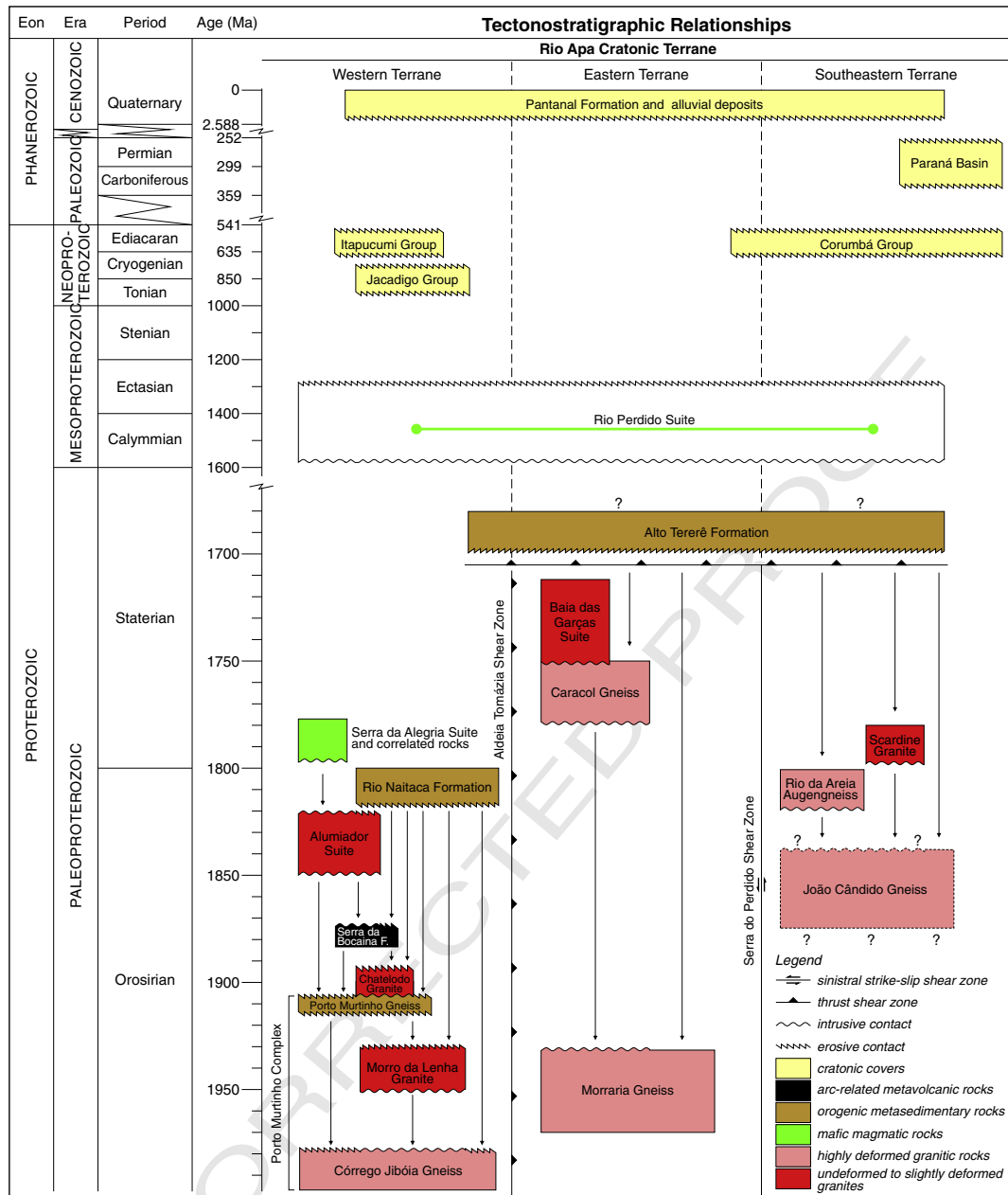


Fig. 7. Columnar sections and flow diagram showing the accretionary history of the Rio Apa Cratonic Terrane.

734 same deformation affected the Alto Tererê Formation, which displays a
 735 Barrovian-type metamorphism with conditions varying from upper
 736 greenschist facies (garnet zone) to middle amphibolite facies (kyanite
 737 zone) (Faleiros et al., 2014; Pavan and Faleiros, 2014; Pavan et al.,
 738 2014). The overall deformational-metamorphic pattern of the Eastern
 739 Terrane characterizes a thick-skin deformation, even though this
 740 terrane is composed of significantly younger units in relation to the
 741 Western Terrane. The contact relationships between the Alto Tererê
 742 Formation with the basement rocks are exclusively characterized by
 743 zones of ultramylonites and phyllonites (Remédio and Faleiros, 2014).
 744 The contact zone between the Western and Eastern Terranes was defined
 745 by the Aldeia Tomázia low-angle top-to-west thrust zone, which was
 746 responsible for a metamorphic inversion, where deeper rocks of the
 747 Eastern Terrane override shallower rocks of the Western Terrane.

748 The available geological and geochronological data (Table 2) indicate
 749 that the Southeastern Terrane is composed of mylonitic banded
 750 gneisses of unknown ages (João Cândido Gneiss) intruded by granitic

751 plutons in the period from 1810 to 1790 Ma. These rocks are covered
 752 by metasedimentary rocks of the Alto Tererê Formation and display de-
 753 formational and metamorphic characteristics very similar to the Eastern
 754 Terrane. A distinct feature is that the Eastern and Southeastern Terranes
 755 are separated by a transcurrent shear zone (Serra do Perdido shear
 756 zone), regionally an uncommon structure.

757 The evidence that the Alto Tererê Formation covers parts of the
 758 Western, Eastern and Southeastern Terranes raises two possible
 759 interpretations: (i) the Alto Tererê Formation is a para-autochthonous
 760 unit deposited over the juxtaposed terranes, or (ii) the Alto Tererê
 761 Formation is an allochthonous nappe thrust over the juxtaposed
 762 terranes. Detrital zircon U–Pb data presented by Lacerda Filho et al.
 763 (2014) favor the first hypothesis. However, the age of juxtaposition of
 764 the three terranes and of the consolidation of the RACT is somewhat
 765 uncertain. At first, the age of 1589 ± 44 Ma obtained for a dyke of the
 766 Rio Perdido Suite in the Western Terrane could be interpreted as the
 767 maximum age for terrane juxtaposition, as this suite intrudes the entire

RACT. However, field and petrographic evidence indicates that some dykes are deformed and completely replaced by metamorphic assemblages, while others cut the regional structures and terrane contacts (Fig. 2) and are preserved from the regional metamorphism. This evidence suggests that part of the dykes crystallized after the regional metamorphism. The main structure of the RACT is associated with a Barrovian-type regional metamorphism (Pavan and Faleiros, 2014), which is expected for and typically associated with crustal thickening in collisional suture zones (e.g., England and Thompson, 1984). ^{40}Ar – ^{39}Ar and K–Ar data (hornblende, muscovite and biotite) obtained primarily from units of the Eastern and Southeastern Terranes (Fig. 2; Araújo et al., 1982; Cordani et al., 2010a) constrain the age of this regional metamorphism to 1310–1270 Ma (Fig. 8). A monazite U–Pb LA-MC-ICP-MS age of 1308 ± 39 Ma obtained for a biotite–staurolite–kyanite–garnet schist from the Alto Tererê Formation (Lacerda Filho et al., 2014) corroborates this interpretation. However, only two biotite ^{40}Ar – ^{39}Ar data are available for the Western Terrane, both from undeformed samples of the Alumiador Granite (Figs. 2 and 8), and the role of the regional metamorphism in this terrane is somewhat uncertain. We interpret that during 1310–1270 Ma, the RACT was converted into a collisional orogen. The available geochronological data suggest a time span of approximately 400 My. between the last accretionary period and the collisional period. From the present data, we interpret that the juxtaposition between the Western, Eastern and Southeastern Terranes must have occurred during the 1310–1270 Ma collisional event.

5.1. Magmatic and tectonic evolution of the RACT

The zircon U–Pb ages present in Table 2 allow the recognition of four main granitic magmatic events of ages within the intervals 1950–1940 Ma, 1900–1880 Ma, 1840–1790 Ma and 1780–1720 Ma.

The oldest event, at 1950–1940 Ma, was recorded in both the Western and Eastern Terranes, and the associated granitic units (Córrego Jibóia Gneiss, Morro da Lenha Granite and Morraria Gneiss) present the geochemical signature of subduction-related calc-alkaline granites (Faleiros et al., 2014). The second magmatic event (1900–1880 Ma) is represented by intrusive granites (Chatelodo Granite; this work) and medium- to high-K calc-alkaline volcanism of the Serra da Bocaina Formation (Godoy et al., 2010; Brittes et al., 2013). The geochemical signatures and the association between the rhyolites and andesites strongly suggest a subduction-related arc magmatism in this period. This magmatic event was only identified in the westernmost portion of the Western Terrane.

The third magmatic event (1840–1790 Ma) was identified in the Western Terrane (Alumiador Suite) and the Southeastern Terrane (Rio da Areia Augen Gneiss and Scardine Granite). In both cases, this event

can be subdivided into two distinct tectonic periods based on U–Pb geochronological determinations (Table 2) and available geochemical data (Silva, 1998; Lacerda Filho et al., 2006; Manzano et al., 2012; Manzano, 2013; Remédio et al., 2014). The Alumiador Granite (1840 Ma) and the Rio da Areia Augen Gneiss (1810 Ma) present arc-like high-K calc-alkaline signatures, and the Santa Otilia (1830 Ma) and Scardine (1790 Ma) Granites exhibit alkaline signatures of extensional settings. Manzano et al. (2012) describe granitic facies of the Alumiador Suite with petrographic and geochemical characteristics of syncollisional granitic series, but these rocks were not dated until now. Although showing the same magmatic and geochronological patterns, the Western and Southeastern Terranes are separated by a 15–60-km-wide intensely deformed zone with distinct geochronological characteristics (the Eastern Terrane), and the two terranes may not have belonged to the same magmatic arc. Sample MS-29A, with an age of 1841 ± 15 Ma (Córrego do Cervo Granite), is located along the contact zone between the Western and Eastern Terranes. This sample represents a granite related to the main accretionary period of the third magmatic event, and it was intensely sheared during the tectonic collage between the two terranes. Rocks from the third magmatic event were only deformed in terrane contact zones.

The fourth magmatic event (1780–1720 Ma) is represented by the whole Eastern Terrane and includes the Caracol Gneiss (1774 ± 26 Ma, Cordani et al., 2010a, 2010b; 1781 ± 7 and 1753 ± 13 Ma, this work) and the Baía das Garças Suite (1754 ± 42 Ma; Cordani et al., 2010a, 2010b), including the Cerro Porã Granite (1749 ± 45 Ma; Plens et al., 2013), the Santa Clarinha Orthogneiss (1750 ± 9 ; this work), the Sanga Bonita Granite (1721 ± 25 ; Cordani et al., 2010a, 2010b) and the Espinilho Orthogneiss (1719 ± 11 ; this work). The latter three units present subduction-related high-K calc-alkaline signatures, suggesting a younger accretionary magmatic event, while the Caracol Gneiss and the Cerro Porã Granite are dominated by alkaline signatures of extensional settings. A distinct characteristic of these magmatic rocks is a generalized strong mylonitic deformation primarily related to westward thrusting. Microstructural evidence, with generalized dynamic recrystallization of quartz by grain boundary migration and incipient recrystallization of feldspar by bulging recrystallization (Table 1), indicates deformational temperatures of approximately 500°C (Voll, 1980; Stipp et al., 2002; Passchier and Trouw, 2005; Faleiros et al., 2010). Superposed brittle deformation of feldspars and bulging recrystallization of quartz indicate that the mylonitization progressed to upper crustal levels during the exhumation of the Eastern Terrane rocks. Bulging recrystallization of quartz generally occurs between 300 and 400°C (Stipp et al., 2002; Faleiros et al., 2010).

Considering that the four granitic events are primarily associated with distinct tectonostratigraphic terranes and are bounded by shear zones, the RACT can be explained as the collage of a series of fragmented diachronic magmatic arcs and other tectonic assemblages in a long-lived accretionary margin, reflecting an extremely mobile tectonic regime. Nevertheless, the spatial relationships of the three younger magmatic events present in the Western and Eastern Terranes display a clear geochronological zonation, which could reflect partially preserved paleogeography. This zonation suggests a magmatic arc with an age of 1900–1880 Ma in the westernmost part of the RACT, followed by a magmatic arc with an age of 1840–1810 Ma in the central part, and a magmatic arc with an age of 1780–1720 Ma in the eastern part of the RACT. This geochronological zonation suggests orogen migration due to progressive subduction from east to west, with subduction of the east plate under the west plate (present-day coordinates).

The metamorphic and structural patterns of the Alto Tererê Formation are consistent with westward crustal thickening during the collisional phase of the orogen (from 1310 to 1270 Ma), and the Alto Tererê Formation could represent a reworked accretionary prism. Barrovian metamorphism suggests collision with an unknown continental mass located to the east between 1310 and 1270 Ma (as indicated by ^{40}Ar – ^{39}Ar hornblende, muscovite and biotite cooling ages

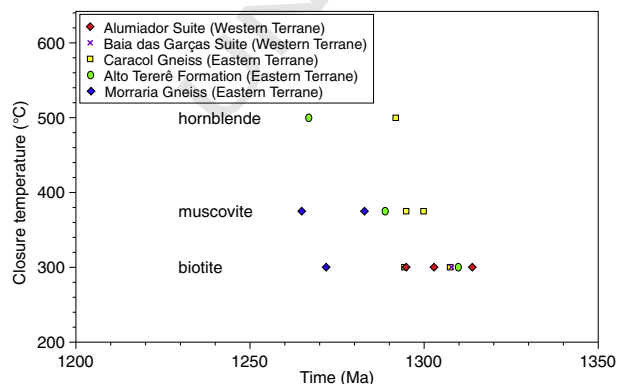


Fig. 8. ^{40}Ar – ^{39}Ar and K–Ar thermochronological data available for rocks of the Rio Apa Cratonic Terrane (Araújo et al., 1982; Cordani et al., 2010a).

879 presented by Cordani et al., 2010a, 2010b, and a U–Pb monazite age
880 presented by Lacerda Filho et al., 2014). The geochronological and
881 geological data suggest a complex composite accretionary orogen of
882 approximately 230 Ma duration (from 1950 to 1720 Ma) that was con-
883 verted into a collisional orogen between 1310 and 1270 Ma.

884 5.2. Relationship to the Amazonian Craton

885 An evaluation of the relationship between the RACT and the
886 Amazonian Craton must first take into account two possibilities: was the
887 RACT autochthonous or allochthonous to the Amazonian Craton in
888 pre-Gondwana times? These two hypotheses are discussed below.

889 5.2.1. RACT autochthonous to the Amazonian Craton

890 The hypothesis of the RACT as autochthonous to the Amazonian
891 Craton implies that the RACT should be a prolongation of the Paraguá
892 Terrane (eastern Bolivia) or Jauru Terrane (Mato Grosso and Rondônia,
893 Brazil). Both possibilities imply that the Grenvillian-age belts (Nova
894 Brasilândia, Aguapeí and Sunsás) should be intracontinental features,
895 as interpreted by Santos et al. (2000, 2008). However, the available
896 U–Pb geochronological data indicate that the basement of the Paraguá
897 and Jauru Terranes is dominated by rocks younger than the RACT
898 basement.

899 The Paraguá Terrane basement is dominated by metasedimentary
900 rocks of the La Chiquitania and San Ignacio Groups, both deposited at
901 or after ca. 1690 Ma. These two groups were intruded by granitic rocks
902 of the Lomas Maneches Suite between 1690 and 1640 Ma (Litherland
903 et al., 1989; Boger et al., 2005; Santos et al., 2008; Vargas-Mattos et al.,
904 2011). Restricted older basement rocks were identified in the southern-
905 most portion of eastern Bolivia: the granulitic orthogneiss of the Lomas
906 Maneches Suite, with a zircon U–Pb age of 1818 ± 13 Ma (Santos et al.,

2008), and the Correrca Granite, with zircon U–Pb ages of $1925 \pm$ 907
 32 Ma and 1894 ± 13 Ma (Vargas-Mattos et al., 2010, 2011). The 908
basement rocks were intruded by voluminous syn-tectonic granites 909
primarily in the period from 1350 to 1320 Ma (Boger et al., 2005; 910
Santos et al., 2008; Matos et al., 2009). Nd isotope data (Lacerda Filho 911
et al., 2006; Santos et al., 2008; Matos et al., 2009; Cordani et al., 912
2010a) indicate that the Paraguá Terrane rocks were primarily derived 913
from a source younger than the RACT source (Nd T_{DM} model ages of 914
1500–2050 Ma against 2000–2600 Ma, respectively; Fig. 9a, b). Thus, 915
besides the youngest rocks, the rocks from the Paraguá Terrane were 916
derived from distinct sources (Fig. 9a–d), which is strong evidence 917
against the correlation between the Paraguá Terrane and the RACT. An 918
exception to this is the Orosirian rocks present in the southernmost por- 919
tion of the eastern Bolivia basement (Correrca Granite; Vargas-Mattos 920
et al., 2010, 2011), which could be interpreted as the northernmost 921
prolongation of the RACT. Furthermore, the Correrca Granite occurs 922
south of the San Diablo Front (Fig. 1), a major sinistral shear zone that 923
is considered the southern boundary of the Sunsas Belt (Litherland 924
et al., 1989). 925

926 Similar to the Paraguá Terrane, the Jauru Terrane is dominated 926
by rocks younger than the RACT (Fig. 9a, b), with granitic suites 927
(e.g., Santa Helena and Rio Branco batholiths) emplaced primarily 928
from 1330 to 1560 Ma (Geraldes et al., 2001; Santos et al., 2008). A re- 929
stricted granitic basement with ages of 1790–1740 Ma was recognized 930
in the Jauru Terrane (Geraldes et al., 2001). The rocks from the Jauru 931
Terrane present Nd T_{DM} model ages between 1350 and 1950 (Fig. 9c, 932
d), indicating that they were not derived from the same source of the 933
RACT, so both terranes cannot be correlated. 934

935 In summary, U–Pb and Nd isotope data (Fig. 9) strongly suggest that 935
the RACT is allochthonous to the SW Amazonian Craton. The implica- 936
tions of this interpretation are discussed in the next section. 937

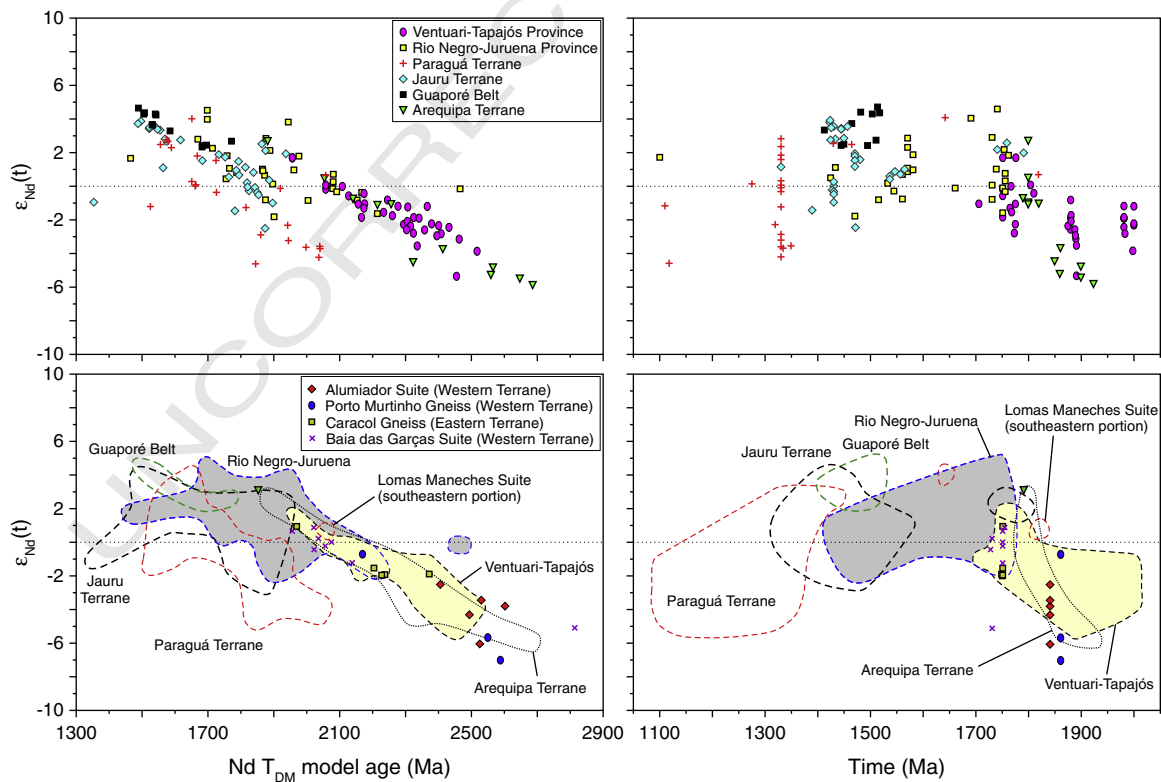


Fig. 9. Sm–Nd whole-rock data compiled from the Rio Apa Cratonic Terrane (Lacerda Filho et al., 2006; Cordani et al., 2010a), the Arequipa Terrane (Bock et al., 2000; Loewy et al., 2004; Casquet et al., 2010) and units from the SW Amazonian Craton: Ventuari–Tapajós Province (Dall’Agnol et al., 1999; Lamarão et al., 2002, 2005; Pinho et al., 2003; Santos et al., 2004), Rio Negro–Juruena Province (Santos et al., 2000, 2008; Payolla et al., 2002), Paraguá Terrane (Santos et al., 2008; Matos et al., 2009), Jauru Terrane (Geraldes et al., 2001; Santos et al., 2008), and Guaporé Belt (Geraldes et al., 2001; Matos et al., 2004).

5.2.2. RACT allochthonous to the Amazonian Craton

If the RACT was allochthonous to the SW Amazonian Craton in pre-Gondwana times, as suggested by available geochronological and isotopic data, two key questions must be answered: (i) Is it possible to recognize the ancestry of the RACT in South America? (ii) When and where did the collage between the RACT and the Amazonian Craton occur?

Based on the age and tectonic setting of the granitic magmatism, Cordani et al. (2010a) correlate the RACT with the Rio-Negro Juruena Province of the Amazonian Craton. In fact, geochemical, U–Pb and Nd isotope data indicate that part of the granitic rocks from the Rio Negro–Juruena Province were formed in an accretionary environment between 1760 and 1730 Ma (Santos et al., 2000; Payolla et al., 2002; Santos et al., 2008), a setting very similar to the Eastern Terrane of the RACT (Fig. 9). This part of the Rio Negro–Juruena Province presents Nd T_{DM} model ages primarily within the 1900–2200 Ma interval (Santos et al., 2000; Payolla et al., 2002; Santos et al., 2008), which coincides with the data of the Eastern Terrane (Lacerda Filho et al., 2006; Cordani et al., 2010a) (Fig. 9). However, the Rio Negro–Juruena accretionary orogen was active until ca. 1500 Ma (Tassinari and Macambira, 1999; Santos et al., 2000; Payolla et al., 2002; Santos et al., 2008), and there are no granitic rocks younger than 1700 Ma in the Eastern Terrane. Furthermore, there are no rocks with U–Pb ages and Nd isotopic signatures similar to those of the Western Terrane of the RACT in the Rio Negro–Juruena Province (Fig. 9). These data make the correlation between the RACT and the Rio Negro–Juruena Province unlikely.

Basement rocks from the Ventuari–Tapajós Province of the Amazonian Craton display U–Pb age and Nd isotopic patterns (Dall'Agnol et al., 1999; Lamarão et al., 2002; Pinho et al., 2003; Santos et al., 2004; Lamarão et al., 2005; Cordani and Teixeira, 2007) that are very similar to the Western and Eastern Terranes (Fig. 9). In this scenario, the RACT can be interpreted as a fragment of the Ventuari–Tapajós Province, which was dispersed and re-incorporated to the proto-Amazonian Craton.

In an alternative model, Casquet et al. (2009, 2010, 2012) correlate the RACT to the Arequipa Terrane (Peru), a correlation that is supported by available U–Pb ages and Nd isotopic patterns (Bock et al., 2000; Loewy et al., 2004; Casquet et al., 2010) (Fig. 9). The existence of the Mara Craton, made up of the Maz Terrane (Western Sierras Pampeanas, Argentina), Arequipa Terrane and the RACT (Casquet et al., 2009, 2012), is a possibility that needs further investigation for confirmation. The Arequipa Terrane records an early magmatism at 1.9–2.1 Ga, an ultrahigh-temperature metamorphism at 1.87 Ga and felsic magmatism at 1.7–1.79 Ga (Casquet et al., 2010). Additionally, the magmatic events can be partially correlated with those recorded in the RACT. Nevertheless, the Arequipa Terrane records a Grenvillian-age low-pressure metamorphism (1.04–0.85 Ga; Casquet et al., 2010), which did not affect the RACT. In the Maz Terrane, magmatic events at 1.9 and 1.7 Ga were only inferred from detrital zircon ages (Casquet et al., 2008).

Considering the RACT as an allochthonous terrane, the history of its collage to the Amazonian Craton should be addressed. As discussed above, geochronological and isotopic data suggest that the RACT does not correlate with the Jauru Terrane and most of the Paraguá Terrane. If we consider the Tucavaca Belt as an aulacogenic feature (Brito Neves et al., 1985; Ávila-Salinas, 1992; Cordani et al., 2009, 2010a), the RACT–Amazonia collage could have occurred during the Rondonian–San Ignacio (1560–1300 Ma) or Grenvillian (1200–1000 Ma) Orogenies. The basement rocks present in the Corumbá region (Fig. 1), which are considered the northernmost exposed portion of the RACT, play a key role in this scenario. Nevertheless, these basement rocks have been very poorly studied. Available thermochronological data are restricted to K–Ar ages of 1730 ± 22 Ma (biotite) and 889 ± 44 Ma (K-feldspar) (Hašui and Almeida, 1970). These data suggest that this basement has not undergone tectonothermal effects related to the Rondonian–San Ignacio event (1560–1300 Ma), and it was possibly little affected by the late Sunsás event, as the closure temperature of K-feldspar to the

argon system can be as low as 150 °C (Lovera et al., 1989). From the present data, we interpret the Sunsás Belt as the most likely suture zone between the RACT and the proto-Amazonian Craton, and the basement south of the San Diablo Front (Bolivia), including the Correraca Granite (Vargas-Mattos et al., 2010, 2011), as the northernmost part of the RACT. In a more regional perspective, the available geological data allow us to interpret the Arequipa Terrane and the RACT as part of a single cratonic mass in pre-Rodinia times.

In a global perspective, accretionary belts with ages concentrated in the period between 1.8 and 1.3 Ga have been reported worldwide and related to the history of growth of the Columbia supercontinent, as observed in the present-day southern margin of North America, Greenland and Baltica, the western margin of the Amazonian Craton, the southern and eastern margins of the North Australia Craton and the southern margin of the North China Craton (Rogers and Santosh, 2002; Zhao et al., 2002, 2004; He et al., 2009; Bettencourt et al., 2010; Zhao et al., 2011; Zhang et al., 2012; Scandolaro et al., 2014). Roberts (2012, 2013) interprets the scarcity of global records of passive margin basins throughout the Mesoproterozoic (Bradley, 2008) as an indication that Columbia did not break up into dispersed continents but remained as a quasi-integral continental lid in the period 1800–1300 Ma. This view is reinforced by a scarcity of evolved Hf signatures in detrital zircons observed worldwide during the period 1700–1200 Ma, which would indicate the absence of interior orogenic belts with high degrees of crustal reworking (Roberts, 2012, 2013). Hf data in detrital zircons indicate an essentially juvenile signature at this period, indicating a dominance of accretionary orogens related to plate margins (Roberts, 2012, 2013), which is consistent with the tectonic scenario of the RACT. Nevertheless, the RACT was not taken into account in recent Columbia reconstructions based on paleomagnetic data (Bispo-Santos et al., 2008, 2012, 2014a, 2014b). The only exception is the Columbia reconstruction presented by Teixeira et al. (2013), where the RACT appears in a marginal position, suggesting that it was part of the proto-Amazonian Craton at ca. 1790 Ma. Based on geological, geochronological and isotopic data, we speculate that between 1950 and 1720 Ma, the RACT, and possibly the Arequipa Terrane, could have been part of the Ventuari–Tapajós Province of the Amazonian Craton, which was subsequently fragmented and dispersed as a microcontinent.

Geological and geochronological data indicate that at the period between 1310 and 1270 Ma, the proto-RACT changed from an accretionary orogen to a collisional orogen, and it was consolidated as a cratonic mass at approximately 1270 Ma, preceding the formation of Rodinia. From 540 Ma, West Gondwana was sectioned by the Transbrasiliano Lineament, an extrusion-related vertical shear zone more than 4500 km long in the NNE–SSW direction (in South America; Fig. 1). This shear zone was responsible for dividing South America into two geotectonic domains: pre-Tonian orogenic belts (Laurentian affinity) to the west and Neoproterozoic orogenic belts (Gondwanan affinity) to the east (Brito Neves and Fuck, 2014). The southern portion of the Transbrasiliano Lineament passes near the present-day eastern boundary of the RACT (Fig. 1). This lineament could be responsible for fragmenting and dispersing the continental mass that collided with the RACT during the event that produced the Barrovian-type metamorphism recorded in the supracrustal rocks of the Eastern and Southeastern Terranes (Alto Tererê Formation), culminating in the loss of an important part of the evolutionary history of the RACT.

6. Uncited reference

Faleiros and Pavan, in preparation

Acknowledgments

Financial support for this work was provided by the Geological Survey of Brazil (CPRM), grants 4220.500 and 4075.500. Eric Tohver

1066 and an anonymous reviewer provided insightful and helpful comments
1067 that improved the resulting contribution. Associate editor Joseph G.
1068 Meert is thanked for his guidance during the editorial process.

1069 Appendix A. Supplementary data

1070 Supplementary data to this article can be found online at <http://dx>.
1071 doi.org/10.1016/j.gr.2015.02.018.

1072 References

- 1073 Araújo, H.J.T., Santos Neto, A., Trindade, C.A.H., Pinto, J.C.A., Montalvão, R.M.G., Dourado,
1074 T.D.C., Palmeira, R.C.B., Tassinari, C.C.G., 1982. Folha SF.21 – Campo Grande: geologia,
1075 geomorfologia, pedologia, vegetação e uso potencial da terra. Levantamento de
1076 Recursos Naturais: Rio de Janeiro, DNPM, Projeto Radam Brasil vol. 28 (416 pp.).
1077 Ávila-Salinas, W., 1992. El magmatismo Cámbrico-Ordovícico em Bolívia. In: Gutierrez
1078 Marco, J.C., Saavedra, J., Rábano, I. (Eds.). Paleozoico Inferior de Ibero-America:
1079 Extremadura. Universidad de Extremadura, pp. 241–253.
1080 Babinski, M., Boggiani, P.C., Fanning, M., Simon, C.M., Sial, A.N., 2008. U–Pb SHRIMP
1081 geochronology and isotope chemostratigraphy (C, O, Sr) of the Tamengo Formation,
1082 southern Paraguay belt, Brazil. VI South American Symposium on Isotope Geology,
1083 San Carlos de Bariloche, Proceedings, p. 160.
1084 Bettencourt, J.S., Leite Jr., W.B., Ruiz, A.S., Matos, R., Payolla, B.L., Tosdal, R.M., 2010. The
1085 Rondonian–San Ignacio Province in the SW Amazonian Craton: an overview. *Journal*
1086 *of South American Earth Sciences* 29, 28–46.
1087 Bispo-Santos, F., D'Agrella-Filho, M.S., Pacca, I.I.G., Janikian, L., Trindade, R.I.F., Elming, S.-Å.,
1088 Silva, J.A., Barros, M.A.S., Pinho, F.E.C., 2008. Columbia revisited: paleomagnetic results
1089 from the 1790 Ma Colider Volcanics (SW Amazonian Craton, Brazil). *Precambrian*
1090 *Research* 164, 40–49.
1091 Q18 Bispo-Santos, F., D'Agrella-Filho, Trindade, R.I.F., Elming, S.-A., Janikian, L., Vasconce-los,
1092 P.M., Perillo, Pacca, I.I.G., Silva, J.A., Barros, M.A.S., 2012. Tectonic implications of the
1093 1419 Ma Nova Guarita mafic intrusives paleomagnetic pole (Amazonian Craton) on
1094 the longevity of Nuna. *Precambrian Research* 196–197, 1–22.
1095 Bispo-Santos, F., D'Agrella-Filho, M.S., Janikian, L., Reis, N.J., Trindade, R.I.F., Reis, M.A.A.,
1096 2014a. Towards Columbia: paleomagnetism of 1980–1960 Ma Surumu volcanic
1097 rocks, Northern Amazonian Craton. *Precambrian Research* 244, 123–138.
1098 Q19 Bispo-Santos, F., D'Agrella-Filho, M.S., Trindade, R.I.F., Janikian, L., Reis, N.J., 2014b. Was
1099 there SAMBA in Columbia? Paleomagnetic evidence from 1790 Ma Avanavero
1100 mafic sills (Northern Amazonian Craton). *Precambrian Research* 244, 139–155.
1101 Bock, B., Bahlburg, H., Wörner, G., Zimmermann, U., 2000. Tracing crustal evolution in the
1102 southern central Andes from Late Precambrian to Permian with geochemical and Nd
1103 and Pb isotope data. *The Journal of Geology* 108, 515–535.
1104 Boger, S.D., Raetz, M., Giles, D., Etchart, E., Fanning, M.C., 2005. U–Pb age data from the
1105 Sundas region of Eastern Bolivia, evidence for the allochthonous origin of the Paragua
1106 Block. *Precambrian Research* 139, 121–146.
1107 Boggiani, P.C., 1997. Análise Estratigráfica da Bacia Corumbá (Neoproterozóico) – Mato
1108 Grosso do Sul. Tese de Doutorado, Instituto de Geociências, Universidade de São
1109 Paulo (181 pp.).
1110 Bradley, D.C., 2008. Passive margins through earth history. *Earth-Science Reviews* 91,
1111 1–26.
1112 Brito Neves, B.B., Fuck, R.A., 2014. The basement of the South American platform: half
1113 Laurentian (N–NW) + half Gondwanan (E–SE) domains. *Precambrian Research*
1114 244, 75–86.
1115 Brito Neves, B.B., Campos Neto, M.C., Cordani, U.G., 1985. Ancient “massifs” in the
1116 Proterozoic belts of Brasil. Symposium on Early to Middle Proterozoic Fold Belts,
1117 1985, Darwin. Extended Abstracts, 1985 vol. 1, pp. 70–72.
1118 Brittes, A.F.N., Sousa, M.Z.A., Ruiz, A.S., Batata, M.E.F., Lafon, J.-M., Plens, D.P., 2013.
1119 Geology, petrology and geochronology (Pb–Pb) of the Serra da Bocaina Formation:
1120 evidence of an Orosirian Amoguijá Magmatic Arc in the Rio Apa Terrane, south of
1121 the Amazonian Craton. *Brazilian Journal of Geology* 43, 48–69.
1122 Bühn, B., Pimentel, M.M., Matteini, M., Dantas, E.L., 2009. High spatial resolution analysis
1123 of Pb and U isotopes for geochronology by laser induced multi-collector inductively
1124 coupled plasma mass spectrometry (LA-MC-IC-MS). *Anais da Academia Brasileira*
1125 *de Ciências* 81, 1–16.
1126 Campanha, G.A.C., Warren, L., Boggiani, P.C., Grohmann, C.H., Cáceres, A.A., 2010. Structural
1127 analysis of the Itapucumí Group in the Vallemi region, northern Paraguay: evidence
1128 of a new Brasiliano/Pan-African mobile belt. *Journal of South American Earth Sciences*
1129 30, 1–11.
1130 Campanha, G.A.C., Boggiani, P.C., Sallun Filho, W., Sá, F.R., Zuquim, M.P.S., Piacentini, T.,
1131 2011. A Faixa de Dobramento Paraguai na Serra da Bodoquena e Depressão do Rio
1132 Miranda, Mato Grosso do Sul. *Geologia USP – Série Científica* 11, pp. 79–96.
1133 Casquet, C., Pankhurst, R.J., Rapela, C.W., Galindo, C.M., Fanning, C.M., Chiaradia, M., Baldo,
1134 E., González-Casado, J.M., Dahlquist, J.A., 2008. The Mesoproterozoic Maz Terrane in
1135 the Western Sierras Pampeanas, Argentina, equivalent to the Arequipa–Antofalla
1136 block of southern Peru? Implications for West Gondwana margin evolution.
1137 *Gondwana Research* 13, 163–175.
1138 Casquet, C., Rapela, C.W., Pankhurst, R.J., Baldo, E., Galindo, C., Fanning, M., Saavedra, J.,
1139 2009. Proterozoic in southern South America: accretion to Amazonia, involvement
1140 in Rodinia formation and further west Gondwana accretion. Rodinia: Superconti-
1141 nents, Superplumes & Scotland. Geological Society, London, Ferrom Meeting,
1142 Edinburgh, Abstract.

- Casquet, C., Fanning, C.M., Galindo, C., Pankhurst, R.J., Rapela, C.W., Torres, P., 2010. The
1143 Arequipa Massif of Peru: new SHRIMP and isotope constraints on a Paleoproterozoic
1144 inlier in the Grenvillian orogen. *Journal of South American Earth Sciences* 29,
1145 128–142.
1146 Casquet, C., Rapela, C.W., Pankhurst, R.J., Baldo, E.G., Galindo, C., Fanning, C.M., Dahlquist,
1147 J.A., Saavedra, J., 2012. A history of Proterozoic terranes in southern South America:
1148 From Rodinia to Gondwana. *Geoscience Frontiers* 3, 137–145.
1149 Cordani, U.G., Teixeira, W., 2007. Proterozoic accretionary belts in the Amazonian Craton.
1150 *Geological Society of America Memoirs* 200, 297–320.
1151 Cordani, U.G., Teixeira, W., D'Agrella-Filho, M.S., Trindade, R.I., 2009. The position of the
1152 Amazonian Craton in supercontinents. *Gondwana Research* 15, 396–407.
1153 Cordani, U.G., Teixeira, W., Tassinari, C.C.G., Coutinho, J.M.V., Ruiz, A.S., 2010a. The Rio Apa
1154 Craton in Mato Grosso do Sul (Brazil) and Northern Paraguay: geochronological
1155 evolution, correlations and tectonic implications for Rodinia and Gondwana.
1156 *American Journal of Science* 310, 981–1023.
1157 Cordani, U.G., Fraga, L.M., Reis, N., Tassinari, C.C.G., Brito-Neves, B.B., 2010b. On the origin
1158 and tectonic significance of the intra-plate events of the Grenvillian-type age in South
1159 America: a discussion. *Journal of South American Earth Sciences* 29, 143–159.
1160 Corrêa, J.A., Correia Filho, F.C.L., Scislowski, G., Neto, C., Cavallon, L.A., Cerqueira, N.L.S.,
1161 Nogueira, V.L., 1976. Projeto Bodoquena: Relatório Final. Goiânia: Convênio DNPM/
1162 CPRM, 8 vTexto integrado, ilustrações e mapas.
1163 Correia Filho, F.C.L., Martins, E.G., Araújo, E.S., 1981. Projeto Rio Apa: Relatório da Área I.
1164 Goiânia: Convênio CODESUL/CPRM vol. 1 (152 pp. Texto, ilustrações e mapas).
1165 Dall'Agnol, R., Costi, H.T., Leite, A.A.S., Magalhães, M.S., Teixeira, N.P., 1999. Rapakivi
1166 granites from Brazil and adjacent areas. *Precambrian Research* 95, 9–39.
1167 England, P.C., Thompson, A.B., 1984. Pressure–temperature–time path of regional
1168 metamorphism I. Heat transfer during evolution of regions of thickened continental
1169 crust. *Journal of Petrology* 25, 894–928.
1170 Faleiros, F.M., Pavan, M., in preparation. Programa Geologia do Brasil – PGB. Geologia e
1171 Recursos Minerais das Folhas Aldeia Tomázia – SF.21-V-B-VI e Fazenda Santa Otília –
1172 SF.21-V-D-III, Estado de Mato Grosso do Sul, Escala 1:100.000. São Paulo: CPRM.
1173 Faleiros, F.M., Campanha, G.A.C., Bello, R.M.S., Fuzikawa, K., 2010. Quartz recrystallization
1174 regimes, c-axis texture transitions and fluid inclusion reequilibration in a prograde
1175 greenschist to amphibolite facies mylonite zone (Ribeira Shear Zone, SE Brazil).
1176 *Tectonophysics* 485, 193–214.
1177 Faleiros, F.M., Caltabeloti, F.P., Pinto, L.G.R., 2013. Programa Geologia do Brasil – PGB.
1178 Aldeia Tomázia. Folha SF.21-V-B-VI. Estado de Mato Grosso do Sul. Carta Geológica
1179 Preliminar. São Paulo: CPRM, 2013, 1 mapa colorido. Escala 1:100.000.
1180 Faleiros, F.M., Caltabeloti, F.P., Pinto, L.G.R., 2014. Programa Geologia do Brasil – PGB.
1181 Aldeia Tomázia. Folha SF.21-V-B-VI. Estado de Mato Grosso do Sul. Carta Geológica.
1182 São Paulo: CPRM, 2014, 1 mapa colorido, 95 × 70 cm. Escala 1:100.000.
1183 Geraldes, M.C., Figueiredo, B.R., Tassinari, C.C.G., Ebert, H.D., 1997. Middle Proterozoic
1184 vein-hosted gold deposits in the Pontes e Lacerda region, southwestern Amazonian
1185 Craton, Brazil. *International Geology Review* 39, 438–448.
1186 Geraldes, M.C., van Schmus, W.R., Condie, K.C., Bell, S., Teixeira, W., Babinski, M., 2001.
1187 Proterozoic geologic evolution of the SW part of the Amazonian craton in Mato
1188 Grosso state, Brazil. *Precambrian Research* 111, 91–128.
1189 Geraldes, M.C., Nogueira, C., Vargas-Mattos, G., Matos, R., Teixeira, W., Valencia, V., Ruiz, J.,
1190 2014. U–Pb detrital zircon ages from the Aguaapé Group (Brazil): implications for
1191 the geological evolution of the SW border of the Amazonian Craton. *Precambrian*
1192 *Research* 244, 306–316.
1193 Godoi, H.O., Martins, E.G., Mello, J.C.R., 2001. Programa Levantamentos Geológicos do
1194 Brasil – PLGB. Corumbá – Folha SE.21-Y-D, Aldeia Tomázia – Folha SF.21-V-B,
1195 Porto Murtinho – Folha SF.21-V-D, Estado de Mato Grosso do Sul. Escala 1:250.000.
1196 Brasília: CPRM/DIEDIG/DEPAT. 65 p., ilustrações e mapas. 1 CD-ROM. (available at
1197 <http://www.cprm.gov.br>).
1198 Godoy, A.M., Manzano, J.C., Araújo, L.M.B., Silva, J.A., 2009. Contexto geológico e estrutural
1199 do Maciço Rio Apa, sul do Cráton Amazoniano – MS. *Geociências* 29, 571–587.
1200 Godoy, A.M., Manzano, J.C., Araújo, L.M.B., Silva, J.A., 2010. Suíte Vulcânica Serra da
1201 Bocaina, Grupo Amoguijá, Maciço Rio Apa – MS. *Geociências* 28, 485–499.
1202 Hasui, Y., Almeida, F.F.A., 1970. Geocronologia do Centro-Oeste Brasileiro. Boletim da
1203 Sociedade Brasileira de Geologia 19, 5–26.
1204 He, Y., Zhao, G., Sun, M., Xia, X., 2009. SHRIMP and LA-ICP-MS zircon geochronology of the
1205 Xiong'er volcanic rocks: implications for the Paleo-Mesoproterozoic evolution of the
1206 southern margin of the North China Craton. *Precambrian Research* 168, 213–222.
1207 Lacerda Filho, J.V., Brito, R.S.C., Silva, M.G., Oliveira, C.C., Moreton, L.C., Martins, E.G., Lopes,
1208 R.C., Lima, T.M., Larizatti, J.H., Valente, C.R., 2006. Geologia e Recursos Minerais do
1209 Estado de Mato Grosso do Sul, Programa Integração, Atualização e Difusão de
1210 Dados da Geologia do Brasil: Convênio CPRM/SEPROTUR/MS, Campo Grande, 121,
1211 escala 1:1000000.
1212 Lacerda Filho, J.V., Fuck, R.A., Ruiz, A.S., Dantas, E.L., Sousa, M.Z.A., Matos, J.B., Nascimento,
1213 N.D.C., 2014. Geologia, geoquímica, geocronologia (U–Pb) e evolução tectônica dos
1214 anfíbolitos do Grupo Alto Tererê, Terreno Rio Apa, Mato Grosso do Sul. *Anais do*
1215 *47º Congresso Brasileiro de Geologia, Salvador*, p. 1522.
1216 Lamarão, C.N., Dall'Agnol, R., Lafon, J.-M., Lima, E.F., 2002. Geology, geochemistry and
1217 Pb–Pb zircon geochronology of the Paleoproterozoic magmatism of Vila Riozinho,
1218 Tapajós gold province, Amazonian craton, Brazil. *Precambrian Research* 119,
1219 189–223.
1220 Lamarão, C.N., Dall'Agnol, R., Pimentel, M.M., 2005. Nd isotopic composition of
1221 Paleoproterozoic volcanic and granitoid rocks of Vila Riozinho: implications for the
1222 crustal evolution of the Tapajós gold province, Amazon craton. *Journal of South*
1223 *American Earth Sciences* 18, 277–292.
1224 Lima, G.A., Souza, M.Z.A., Ruiz, A.S., D'Agrella-Filho, M.S., Vasconcelos, P., 2012. Sills
1225 máficos da Suíte Intrusiva Huanchaca-SW do Cráton Amazoniano: registro de
1226 magmatismo fissural relacionado à ruptura do Supercontinente Rodinia. *Revista*
1227 *Brasileira de Geociências* 42, 111–129.

- Litherland, M., Annells, R.N., Darbyshire, D.P.F., Fletcher, C.J.N., Hawkins, M.P., Klinck, B.A., Mitchell, W.I., O'Connor, E.A., Pitfield, P.E.J., Power, G., Webb, B.C., 1989. The Proterozoic of eastern Bolivia and its relationship to the Andean mobile belt. *Precambrian Research* 43, 157–174.
- Loewy, S.L., Connelly, J.N., Dalziel, W.D., 2004. An orphaned basement block: the Arequipa–Antofalla Basement of the central Andean margin of South America. *Geological Society of America Bulletin* 116, 171–187.
- Lovera, O.M., Richter, F.M., Harrison, T.M., 1989. The $^{40}\text{Ar}/^{39}\text{Ar}$ thermochronometry for slowly cooled samples having a distribution of diffusion domain sizes. *Journal of Geophysical Research* 94, 17917–17935.
- Ludwig, K.R., 2003. *Isoplot 3.00 – a geochronological toolkit for Microsoft Excel*. Berkeley Geochronology Center, Special Publication No 4.
- Manzano, J.C., 2013. *Evolução do Terreno Rio Apa e sua relação com a Faixa de Dobramentos Paraguai*. Tese de Doutorado, Instituto de Geociências e Ciências Exatas, Universidade Estadual Paulista (150 pp.).
- Manzano, J.C., Godoy, A.M., Araújo, L.M.B., Godoy, L.P., 2012. Suíte Plutônica Alumiador, Grupo Amoguijá, Maciço Rio Apa – MS. *Geociências* 31, 351–370.
- Matos, J.B., Schorscher, J.H.D., Geraldés, M.C., Souza, M.Z.A., Ruiz, A.S., 2004. Petrografia, geoquímica e geocronologia das rochas do Orógeno Rio Alegre, Mato Grosso: Um registro de crosta oceânica mesoproterozóica no SW do Cráton Amazônico. *Geologia USP – Série Científica* 4, pp. 75–90.
- Matos, R., Teixeira, W., Geraldés, M.C., Bettencourt, J.S., 2009. Geochemistry and isotopic evidence of the Pensamiento Granitoid Complex, Rondonian–San Ignacio province, eastern Precambrian Shield of Bolivia: petrogenetic constraints for a Mesoproterozoic magmatic arc setting. *Geologia USP – Série Científica* 9, pp. 89–117.
- Meert, J.G., 2002. Paleomagnetic evidence for a Paleo-Mesoproterozoic supercontinent Columbia. *Gondwana Research* 5, 207–215.
- Meert, J.G., 2014. Strange attractors, spirital interlopers and lonely wanderers: the search for pre-Pangæan supercontinents. *Geoscience Frontiers* 5, 155–166.
- Nogueira, V.L., Oliveira, C.C., Figueiredo, J.A., Correia Filho, F.C.L., Scislowski, G., Souza, M.R., Moraes Filho, J.C.R., Leite, E.A., Souza, N.B., Souza, J.O., Cerqueira, N.L.S., Vanderlei, A.A., Takahashi, A.T., Abreu Filho, W., Rosito, J., Olivatti, O., Hausen, J.E.P., Gonçalves, G.N.D., Ramalho, R., Pereira, L.C.B., 1978. Projeto Bonito Aquidauana: Relatório Final. Goiânia: Convênio DNP/CPRM, 14 v. Relatório do Arquivo Técnico da DGM 2.744.
- Passchier, C.W., Trouw, R.A.J., 2005. *Microtectonics*. 2nd edition. Springer-Verlag, Heidelberg, Berlin (366 pp.).
- Pavan, M., Faleiros, F.M., 2014. Geologia da borda W do Terreno Rio Apa, SE do Cráton Amazônico, SW do Mato Grosso do Sul. *Anais do 47º Congresso Brasileiro de Geologia, Salvador*, p. 1668.
- Pavan, M., Caltabeloti, F.P., Pinto, L.G.R., 2014. Programa Geologia do Brasil – PGB. Fazenda Santa Otilia. Folha SF.21-V-D-III. Estado de Mato Grosso do Sul. Carta Geológica. São Paulo: CPRM, 2014, 1 mapa colorido, 95 × 70 cm. Escala 1:100.000.
- Payolla, B.L., Bettencourt, J.S., Kozuch, M., Leite Jr., W.B., Fetter, A.H., Van Schmus, W.R., 2002. Geological evolution of the basement rocks in central part of Rondônia Tin Province, SW Amazonian craton, Brazil: U–Pb and Sm–Nd isotopic constraints. *Precambrian Research* 119, 141–169.
- Pinho, M.A.S.B., Chemale Júnior, F., Van Schmus, W.R., Pinho, F.E.C., 2003. U–Pb and Sm–Nd evidence for 1.76–1.77Ga magmatism in the Morerú region, Mato Grosso, Brazil: implications for province boundaries in the SW Amazonian Craton. *Precambrian Research* 126, 1–25.
- Pinto-Azevedo, E.J.H.C.B., Caltabeloti, F.P., Pinto, L.G.R., 2014. Programa Geologia do Brasil – PGB. Colônia São Lourenço. Folha SF.21-V-D-VI. Estado de Mato Grosso do Sul. Carta Geológica. São Paulo: CPRM, 2014, 1 mapa colorido, 95 × 70 cm. Escala 1:100.000.
- Plens, D.P., Ruiz, A.S., Sousa, M.Z.A., Batata, M.E.F., Lafon, J.-M., Brittes, A.F.N., 2013. Cerro Porã Batholith: post-orogenic A-type granite from the Amoguijá Magmatic Arc – Rio Apa Terrane – South of the Amazonian Craton. *Brazilian Journal of Geology* 43, 515–534.
- Remédio, M.J., Faleiros, F.M., 2014. Programa Geologia do Brasil – PGB. Geologia e Recursos Minerais da Folha Fazenda Margarida – SF.21-X-C-IV, Estado de Mato Grosso do Sul, Escala 1:100.000. São Paulo: CPRM, 2014.
- Remédio, M.J., Costa, V.S., Almeida, V.V., Pinto-Azevedo, E.J.H.C.B., Ferrari, V.C., Brumatti, M., Pinto, L.G.R., Caltabeloti, F.P., Faleiros, F.M., 2013. Programa Geologia do Brasil – PGB. Fazenda Margarida. Folha SF.21-X-C-IV. Estado de Mato Grosso do Sul. Carta Geológica. São Paulo: CPRM, 2013, 1 mapa colorido, 95 × 70 cm. Escala 1:100.000.
- Remédio, M.J., Faleiros, F.M., Brumatti, M., Almeida, V.V., Costa, V.S., 2014. Unidades Litoestratigráficas. In: Remédio, M.J., Faleiros, F.M. (org.), Programa Geologia do Brasil – PGB. Geologia e Recursos Minerais da Folha Fazenda Margarida – SF.21-X-C-IV, Estado de Mato Grosso do Sul, Escala 1:100.000. São Paulo: CPRM, 2014.
- Rizzotto, G.J., Santos, J.O.S., Hartmann, L.A., Tohver, E., Pimentel, M.M., McNaughton, N.J., 2013. The Mesoproterozoic Guaporé suture in the SW Amazonian Craton: geotectonic implications based on field geology, zircon geochronology and Nd–Sr isotope geochemistry. *Journal of South American Earth Sciences* 48, 271–295.
- Rizzotto, G.J., Hartmann, L.A., Santos, J.O.S., McNaughton, N.J., 2014. Tectonic evolution of the southern margin of the Amazonian craton in the late Mesoproterozoic based on field relationships and zircon U–Pb geochronology. *Anais da Academia Brasileira de Ciências* 86, 57–84.
- Roberts, N.M.W., 2012. Increased loss of continental crust during supercontinent amalgamation. *Gondwana Research* 21, 994–1000.
- Roberts, N.M.W., 2013. The boring billion? – Lid tectonics, continental growth and environmental change associated with the Columbia supercontinent. *Geoscience Frontiers* 4, 681–691.
- Rogers, J.J.W., Santosh, M., 2002. Configuration of Columbia, a Mesoproterozoic supercontinent. *Gondwana Research* 5, 5–22.
- Ruiz, A.S., Simões, L.S.A., Brito Neves, B.B., 2005. Maciço Rio Apa: extremo meridional do Cráton Amazônico. *Simpósio Nacional de Estudos Tectônicos – SNET*, 10, 2005. Curitiba. SBG, Anais... Curitiba, pp. 301–304 (2005).
- Sadowski, G.R., Bettencourt, J.S., 1996. Mesoproterozoic tectonic correlations between eastern Laurentia and the western border of the Amazonian Craton. *Precambrian Research* 76, 213–227.
- Saes, G.S., 1999. *Evolução Tectônica e Paleogeográfica do Aulacógeno Aguapeí (1.2–1.0 Ga) e dos Terrenos do seu Embasamento na Porção Sul do Cráton Amazônico*. PhD Thesis, Instituto de Geociências, Universidade de São Paulo (137 pp.).
- Santos, J.O.S., Hartmann, L.A., Gadette, H.E., Groves, D.L., McNaughton, N.J., Fletcher, I.R., 2000. A new understanding of the provinces of the Amazon craton based on integration of field mapping and U–Pb and Sm–Nd geochronology. *Gondwana Research* 3, 453–488.
- Santos, J.O.S., Rizzotto, G.J., Potterd, P.E., McNaughton, N.J., Matos, R., Hartmann, L.A., Chemale Jr., F., Quadros, M.L.E.S., 2008. Age and autochthonous evolution of the Sunsás Orogen in West Amazon Craton based on mapping and U–Pb geochronology. *Precambrian Research* 165, 120–152.
- Scandolara, J.E., Ribeiro, P.S.E., Frasca, A.A.S., Fuck, R.A., Rodrigues, J.B., 2014. Geochemistry and geochronology of mafic rocks from the Vespour suite in the Jurueña arc, Roosevelt–Jurueña terrain, Brazil: implications for Proterozoic crustal growth and geodynamic setting of the SW Amazonian Craton. *Journal of South American Earth Sciences* <http://dx.doi.org/10.1016/j.jsames.2014.04.001>.
- Silva, E.L., 1998. Geologia da região da Serra da Alegria, extremo sul do Cráton Amazônico, município de Porto Murтинinho–MS. *Dissertação de Mestrado*, Instituto de Geociências, Universidade de São Paulo (147 pp.).
- Stipp, M., Stünitz, H., Heilbronner, R., Schmid, S.M., 2002. The eastern Tonalé fault zone: a 'natural laboratory' for crystal plastic deformation of quartz over a temperature range from 250 to 700 °C. *Journal of Structural Geology* 24, 1861–1884.
- Tassinari, C.C.G., Macambira, M.J.B., 1999. Geochronological provinces of the Amazonian Craton. *Episodes* 22, 174–182.
- Teixeira, W., D'Agrella-Filho, M.S., Hamilton, M.A., Ernst, R.E., Girardi, V.A.V., Mazzucchelli, M., Bettencourt, J.S., 2013. U–Pb (ID-TIMS) baddeleyite ages and paleomagnetism of 1.79 and 1.59 Ga tholeiitic dyke swarms, and position of the Rio de la Plata Craton within the Columbia supercontinent. *Lithos* 174, 157–174.
- Tohver, E., van der Pluijm, B.A., Mezger, K., Essene, E., Scandolara, J.E., Rizzotto, G.J., 2004. Significance of the Nova Brasilândia metasedimentary belt in Western Brazil: redefining the Mesoproterozoic boundary of the Amazon Craton. *Tectonics* 23, 1–20.
- Tohver, E., van der Pluijm, B.A., Scandolara, J.E., Essene, E., 2005a. Late Mesoproterozoic deformation of SW Amazônia (Rondônia, Brazil): geochronological and structural evidence for collision with Southern Laurentia. *Journal of Geology* 113, 309–323.
- Tohver, E., van der Pluijm, B.A., Scandolara, J.E., Essene, E.J., 2005b. Two stage history of the SW Amazon Craton in the late Mesoproterozoic: identifying a cryptic suture zone. *Precambrian Research* 137, 35–59.
- Tohver, E., Teixeira, W., van der Pluijm, B., Geraldés, M.C., Bettencourt, J.S., Rizzotto, G., 2006. Restored transect across the exhumed Grenville orogen of Laurentia and Amazonia, with implications for crustal architecture. *Geology* 34, 669–672.
- Vargas-Mattos, G., Geraldés, M.C., Matos, R., Teixeira, W., 2010. Paleoproterozoic granites in Bolivian Precambrian shield: the 1.92–1.89 Ga Correrca magmatic rocks and tectonic implications. *VI Simpósio de Geologia Isotópica da Americado Sul, Brasília*, p. 65.
- Vargas-Mattos, G.L., Geraldés, M.C., Matos, R., Teixeira, W., 2011. LA-ICPMS U–Pb ages of Paleo- and Mesoproterozoic granites in Bolivia. *Goldschmidt Conference Abstracts*, p. 2074.
- Voll, G., 1980. Ein Querprofil durch die Schweizer Alpen vom Vierwaldstötter See zur Wurzelzone – Strukturen und ihre Entwicklung durch Deformationsmechanismen wichtiger Mineralite. *Neues Jahrbuch für Geologie und Paläontologie* 160, 321–335.
- Warren, L.V., 2011. Tectônica e sedimentação do Grupo Itapucumi (Neoproterozoico, Paraguai Setentrional). Tese de Doutorado, Instituto de Geociências, Universidade de São Paulo (215 pp.).
- Warren, L.V., Fairchild, T.R., Gaucher, C., Boggiani, P.C., Poiré, D.G., Anelli, L.E., Inchausti, J.C.G., 2011. Corumbella and in situ Cloudina in association with thrombolites in the Ediacaran Itapucumi Group, Paraguay. *Terra Nova* 23, 382–389.
- Williams, I.S., 1998. U–Th–Pb geochronology by ion microprobe. *Reviews in Economic Geology* 7, 1–35.
- Zhang, S., Li, Z.-X., Evans, D.A.D., Wu, H., Li, H., Dong, J., 2012. Pre-Rodinia supercontinent Nuna shaping up: a global synthesis with new paleomagnetic results from North China. *Earth and Planetary Science Letters* 353–354, 145–155.
- Zhao, G., Cawood, P.A., Wilde, S.A., Sun, M., 2002. Review of global 2.1–1.8 Ga orogens: implications for a pre-Rodinia supercontinent. *Earth-Science Reviews* 59, 125–162.
- Zhao, G., Sun, M., Wilde, S.A., Li, S., 2004. A Paleo-Mesoproterozoic supercontinent: assembly, growth and breakup. *Earth-Science Reviews* 67, 91–123.
- Zhao, G., Li, S., Sun, M., Wilde, S.A., 2011. Assembly, accretion, and break-up of the Palaeo-Mesoproterozoic Columbia supercontinent: recording the North China Craton revisited. *International Geology Review* 53, 1331–1356.